

# Three Parton Corrections, Isospin Symmetry, and $B \rightarrow \pi K$ Puzzle

Tsung-Wen Yeh

*Department of Science Education and Application,  
National Taichung University of Education, Taiwan, R.O.C.\**

(Dated: July 22, 2022)

In this work, we study the  $B \rightarrow \pi K$  puzzle by calculating the three parton one loop corrections in the QCD factorization (QCDF) approach. After a factorization analysis for the corrections, we propose a QCDF factorization formula with three parton one loop corrections. Because of their small contributions and soft end-point divergences, we have neglected the annihilation terms. We employ a general parametrization model for the  $B \rightarrow \pi K$  amplitudes to introduce twelve independent parameters, the weak angle  $\gamma$  and the other eleven hadronic parameters. To reduce the number of independent parameters, these eleven parameters are assumed process-independent and obey the isospin symmetry. These parameters are then calculated by the improved QCDF formula. Due to the chirally enhanced feature of the three parton terms at tree and one loop level, the predictions for the branching ratios can almost cover the experimental data within perturbative energy range (assumed  $\frac{1}{2}m_b$  and  $2m_b$  with  $m_b$  the  $b$  quark's mass). It is significantly improved than the two parton calculations. However, the predictions with the isospin symmetry breaking from the mass differences are not enough to explain the puzzle of the direct CP asymmetries. In order to solve this problem, we propose the following dynamical isospin symmetry breaking mechanism. First, the QCDF calculations can afford the perturbative parts of these eleven parameter. The three phase parameters from the gluonic penguin, color suppressed, and color favored tree diagrams contain additional nonperturbative QCD effects. Second, the perturbative parts of these hadronic parameters need to be process-dependent, such that they are functions of the factorization scales,  $\mu_i$ , for different decay modes. Third, these eight unknown parameters, four scale variables, one weak angle, and three nonperturbative strong phases, can be determined by a least square fit to the eight measurements of four branching ratios and four direct CP asymmetries. The fit shows that the model based on QCDF calculations can completely accommodate the experimental data by choosing different factorization scales around  $m_B$ , the  $B$  meson's mass, for different decay modes. To explain the data, the eleven hadronic parameters and the three nonperturbative strong phases are found to be process-dependent. A large negative relative phase associated with the internal up quark gluonic penguin diagram is observed. The weak angle  $\gamma$  is found to be  $72.1 \pm 5.8$  degree, being consistent with the world averaged value,  $72.1 \pm 5.8$  degree. Using the fit data to the mixing induced asymmetry  $S(\pi^0 K_S) = 0.58 \pm 0.06$ , the weak angle  $\beta$  is determined to be  $22.9 \pm 2.1$  degree, in agreement with the world averaged value,  $22.5 \pm 4.4 \pm 0.6$  degree. The theoretical prediction for the ratio  $C'/T'$  (color suppressed/color favored) is found to be  $0.58 \pm 0.12$ . The above evidences indicate that the  $B \rightarrow \pi K$  puzzle can be solved. By the fit data, we may reconstruct the experimental data at the amplitude level. This enables us to examine the underlying isospin symmetry of the  $B \rightarrow \pi K$  system, the quadrangle relation. The ratio of the two sides of the quadrangle relation is calculated to be  $r = (0.87 \pm 0.15) \exp(-i22^\circ)$ , which signals the isospin symmetry breaking at  $6\sigma$ . The nonzero phases and process-dependent amplitude parameters break the isospin symmetry “dynamically”. The generalization of our model by including any New Physics is possible. The application of our method to other decay processes is straightforward.

**PACS numbers:** 12.15.Ff, 12.38.Bx, 12.39.St, 13.25.Hw, 14.40.Nd.

**Keywords:** perturbative QCD, factorization, isospin, B physics, CP violation, CKM mechanism.

## I. INTRODUCTION

In order to establish the CKM mechanism of the Standard Model (SM), the studies of hadronic  $B$  decays have been devoted to construct the unitarity triangle  $V_{ub}^* V_{ud} + V_{cb}^* V_{cd} + V_{tb}^* V_{td} = 0$  [1]. The triangle contains three angles and sides, for which a systematic procedure has been developed [1, 2]. If the CPT is conserved, then the CP violation can happen through the interference of at least two amplitudes with different weak and strong

phases. However, the uncertainties of strong phases make it difficult to extract the weak phases directly. To overcome, many challenging works are required. There include experimental efforts for measuring many rare and CP violating decays, which have very small branching ratios. On the theoretical side, it needs more accurate calculation frameworks for understanding the underlying physics.

In past decades, it has been exciting to have precisely measured many rare processes by the B factories in BABAR and Belle [3]. The benchmarks are the mixing induced CP asymmetry  $S(B \rightarrow J/\psi K) = 0.691 \pm 0.017$  and the direct CP asymmetry  $A_{CP}(B^0 \rightarrow \pi^- K^+) = -0.082 \pm 0.006$  [4]. In the mean while, there appeared

---

\* twyeh@mail.ntcu.edu.tw

many difficulties to explain these results by the SM. One of these stunning issues is the  $B \rightarrow \pi K$  puzzle [5–7], for which new physics (NP) beyond the SM seems unavoidable [5, 7–10].

The  $B \rightarrow \pi K$  puzzle comes from the following facts:

1. The theoretical predictions for the branching ratios are smaller than the experimental data [11–14].
2. The theoretical predictions for the CP asymmetries have a much different pattern from that of the experimental measurements [8, 11–16].
3. It is difficult to reach consistent SM explanations for different experimental measurements [5–7].

According to the above definitions for the puzzle, one possible solution to the  $B \rightarrow \pi K$  puzzle needs to (i) provide sufficient predictions for the branching ratios, (ii) explain how to conciliate the differences between the predicted pattern and the experimental one of the direct CP asymmetries, (iii) show possible generalizations to other measurements.

However, one should note that the inconsistency may not always come from the theories. The inconsistency may exist between different experiments [17–19]. In the claim of the puzzle, one always assumes that different experiments are consistent. But, this may not be completely correct. One should be careful to identify the third item of the puzzle. In this work, only  $B \rightarrow \pi K$  measurements will be considered.

Further more, it is necessary to examine any possible assumption underlying the theories. In our present interest, they are the isospin symmetry and the process-independence of the amplitude parameters. It is known that the weak interactions conserve the isospin symmetry. In addition, the mass differences,  $\Delta m_x = |m_{x_1} - m_{x_2}|$ , with  $(x, x_1, x_2) = (q, d, u), (\pi, \pi^0, \pi^\pm), (K, K^0, K^\pm), (B, B^0, B^\pm)$  are much smaller than the characteristic energy scale,  $m_b \simeq 4.2\text{GeV}$ , the bottom quark’s mass. The isospin symmetry is good for  $B \rightarrow \pi K$  decays [20, 21]. The conservation of isospin charge implies that the decay amplitudes can be expressed in terms of isospin parameters,  $B_{1/2}$ ,  $A_{1/2}$  and  $A_{3/2}$ , where  $I = 1/2(3/2)$  is the absolute value of the eigenvalue of the isospin charge of the final state  $|\pi K\rangle$ . These parameters need to be independent of the decay modes, otherwise the isospin symmetry can not be conserved. Therefore, the isospin symmetry and the process-independence of amplitude parameters are closely correlated. In latter text, we will explore this point.

At present, it seems still unable to solve the puzzle by model-independent methods [22], such as the flavor symmetry approach [5–7, 10, 23], or the global-fit approach [9, 22–25]. The other possible method could be to employ the perturbative QCD (pQCD) theories to calculate the perturbative parts up-to sufficient accuracy and extract the remaining part from the data [8, 16, 26–28]. As a result, it may help to improve our understanding about

the puzzle. Of course, the drawback of this method is that the extracted information may be model dependent. However, this could be unavoidable due to our limited knowledge.

In this work, QCD factorization (QCDF)[11, 29, 30] is employed to construct a framework, which could fulfill the above requirements for a solution. The central concern will be put on how to disentangle the weak phases from the others. Specifically, a minimal model based on the QCDF according to a general parametrization for the  $B \rightarrow \pi K$  decays will be constructed. The minimal means that only the lowest possible extension of the QCDF is made by introducing three relevant phase factors, which are closely related to the direct CP asymmetries. The other extension is possible than this minimal assumption.

By assuming that the SM is correct, the central core of the puzzle could be related to the hadronic matrix element,  $\langle B | H_{eff} | \pi K \rangle$ . Although the matrix element is still not completely calculable, the factorization theorem proven in high energy physics [31, 32] implies that  $\langle B | H_{eff} | \pi K \rangle$  could be factorized into a functional product of the perturbative QCD and nonperturbative QCD parts. Due to color confinement, the nonperturbative QCD is still not within our theoretical capability. On the other hand, the perturbative QCD can be systematically calculated. This conjecture has been proven up-to next-to-leading order (NLO) in  $\alpha_s$ [12, 29, 33]. Based on three different factorization assumptions, there are three different formalism: the QCD factorization (QCDF)[11, 29, 34], the perturbative QCD factorization (PQCD)[13] and the soft collinear effective theory (SCET)[28]. The common fact is that the matrix element can be expressed as a sum of different Feynman diagram amplitudes [34]. Each amplitude is then factorized as a convolution product of the short and long distance parts. The short distance part collects hard scattering contributions, which are calculable by pQCD methods. The long distance part contains nonperturbative QCD physics, which are submitted for models or nonperturbative methods. Although the perturbative parts are process dependent, the pQCD approach has the prediction ability. This is because that, once the nonperturbative parts have been determined, they can be applied for other processes.

From the point of view of the pQCD approach, the matrix element and its amplitude components would be process dependent. The reason is easy to understand, because the amplitude is expressed as the convolution integral of the short and long distance parts. Although the long distance part is process independent, the process dependence of the short distance part makes the amplitude to be process dependent. This means that these objects may not be directly applicable for other processes if they have been determined in some processes. However, the most studies of the  $B \rightarrow \pi K$  puzzle and related phenomena have assumed that these amplitude variables are process independent. They employed a best-fit or fitting strategy to determine the amplitude parameters

in some processes and applied the fitted amplitude parameters to other processes for predictions or extractions of weak phases. As a result, some inconsistent explanations appeared. This may explain how the puzzle could happen. On the other hand, employing pQCD approach may avoid this problem and could provide some hints for solving the puzzle. Since different pQCD formalisms may lead to different explanations, this work only concentrates on how to employ QCDF for investigations.

The progress of QCDF is continuing. The calculations up-to NLO [11] and NNLO [35–37] radiative corrections have been completed. In Ref.[38], the power corrections from radiative corrections, the renormalon, were calculated. In summary, the QCDF calculations in past years have considered corrections up to twist-3 two parton and NNLO in  $\alpha_s$  [11, 36–39]. These calculations show no significant enhancements in the predictions for the branching ratios and direct CP asymmetries, if not including large uncertainties from model dependent end-point divergent terms or input parameters [11].

Since the  $B \rightarrow \pi K$  decays are penguin dominated, there are twist-3 chirally enhanced corrections from the effective operator  $Q_{6,8}$ . At twist-3 order, there exist both two parton and three parton contributions. However, the previous calculations have neglected the three parton terms. As indicated in Ref.[40], if the three parton terms could exist at tree level, then the predictions of branching ratios could be enhanced by at least about 60%. This sheds light on further enhancements by three parton loop corrections. In this work, it will show that if these three parton one loop corrections are considered, then the predictions could fully accommodate the data.

The organization is as follows. In Sec.II, a general parametrization method for the amplitudes based on the diagrammatic method [34, 41] will be used to construct the model for the  $B \rightarrow \pi K$  decays. The model contains twelve parameters: the weak angle  $\gamma$  and the other eleven hadronic parameters. An improved factorization formula up-to  $O(\alpha_s^2/m_b)$  will be introduced by including the three parton tree and one loop corrections. The calculations for the amplitude parameters of the model will be present in Sec.III. In order to disentangle the weak and the strong phases from the data, a fitting strategy will be constructed according to the least square method. This is completed in Sec.IV. According to the fit result, the phenomenology analysis and discussion will be present in Sec.V. Conclusion is given in Sec.VI.

## II. MODEL

### A. Parametrization And Isospin Symmetry

In general, the amplitudes for  $B \rightarrow \pi K$  decays with  $B = B^\pm, B^0(\bar{B}^0)$ ,  $K = K^\pm, K^0(\bar{K}^0)$ , and  $\pi = \pi^\pm, \pi^0$ ,

could be parameterized as follows [11, 22, 34, 41, 42]

$$\begin{aligned} A(\pi^- \bar{K}^0) &= P'(1 + \epsilon_a e^{i\phi_a} e^{-i\gamma}), \\ -\sqrt{2}A(\pi^0 K^-) &= P'(1 + \epsilon_a e^{i\phi_a} e^{-i\gamma} \\ &\quad - \epsilon_{3/2} e^{i\phi} (e^{-i\gamma} - q e^{i\omega})), \\ -A(\pi^+ K^-) &= P'(1 + \epsilon_a e^{i\phi_a} e^{-i\gamma} \\ &\quad - \epsilon_T e^{i\phi_T} (e^{-i\gamma} - q_C e^{i\omega_C})), \\ \sqrt{2}A(\pi^0 \bar{K}^0) &= P'(1 + \epsilon_a e^{i\phi_a} e^{-i\gamma} \\ &\quad + (\epsilon_{3/2} e^{i\phi} - \epsilon_T e^{i\phi_T}) e^{-i\gamma} \\ &\quad + (\epsilon_T q_C e^{i(\phi_T + \omega_C)} - \epsilon_{3/2} q e^{i(\phi + \omega)})), \end{aligned} \quad (1)$$

where  $A(\pi K)$  mean the amplitudes of  $B \rightarrow \pi K$  decays. In the above expressions, the “unitarity triangle” has been used to translate the contributions from  $\lambda_t$  to the  $\lambda_u$  and  $\lambda_c$  terms, where  $\lambda_q = V_{qb}^* V_{qd}$  for  $q = u, c, t$ .  $P'$  denotes the major penguin amplitude (containing  $\lambda_c$ ). The weak angle  $\gamma = \arg(V_{ub}^*)$  comes from the terms containing  $\lambda_u$ . The other factors are real hadronic terms  $\epsilon_a$ ,  $\epsilon_{3/2}$ ,  $\epsilon_T$ ,  $q$  and  $q_C$  and their associated strong phases  $\phi_a$ ,  $\phi$ ,  $\phi_T$ ,  $\omega$ ,  $\omega_C$  [11]. The amplitudes for  $B^{+,0}$  are obtained by replacing the weak angle  $\gamma$  by  $-\gamma$ . Some relative minor terms such as annihilation, exchange and penguin-annihilation terms have been neglected.

In Eq(1), the isospin symmetry is assumed. The initial  $B$  meson ( $B^-$ ,  $\bar{B}^0$ ) is of  $I_B = -\frac{1}{2}$  state  $|B(I = -\frac{1}{2})\rangle$ . The final ( $\pi K$ ) state can be decomposed into the  $I_{\pi K} = +\frac{1}{2}$  state  $\langle \pi(I = 1)K(I = -\frac{1}{2}) |$ , the  $I_{\pi K} = -\frac{1}{2}$  state  $\langle \pi(I = 0)K(I = -\frac{1}{2}) |$ , and the  $I = -\frac{3}{2}$  state  $\langle \pi(I = -1)K(I = -\frac{1}{2}) |$ . The effective weak Hamiltonian has  $\Delta I = 0$  and  $\Delta I = 1$  operators, where  $\Delta I \equiv |I_B - I_{\pi K}|$ . Therefore, the matrix element  $\langle \pi K | H_{eff} | B \rangle$  could be described by three isospin amplitudes  $B_{1/2}$ ,  $A_{1/2}$ , and  $A_{3/2}$ , which correspond to  $\Delta I = 0$  with  $I_{\pi K} = -\frac{1}{2}$ ,  $\Delta I = 1$  with  $I_{\pi K} = +\frac{1}{2}$ ,  $\Delta I = 1$  with  $I_{\pi K} = -\frac{3}{2}$ , respectively. The decay amplitudes are expressed as [22]

$$A(\pi^- \bar{K}^0) = B_{1/2} + A_{1/2} + A_{3/2}, \quad (2)$$

$$-\sqrt{2}A(\pi^0 K^-) = B_{1/2} + A_{1/2} - 2A_{3/2}, \quad (3)$$

$$-A(\pi^+ K^-) = B_{1/2} - A_{1/2} - A_{3/2}, \quad (4)$$

$$\sqrt{2}A(\pi^0 \bar{K}^0) = B_{1/2} - A_{1/2} + 2A_{3/2}, \quad (5)$$

from which the quadrangle relation [20, 21] is obtained

$$\begin{aligned} A(\pi^- \bar{K}^0) + \sqrt{2}A(\pi^0 K^-) \\ = A(\pi^+ K^-) + \sqrt{2}A(\pi^0 \bar{K}^0) \\ = 3A_{3/2}. \end{aligned} \quad (6)$$

These isospin amplitudes  $B_{1/2}$ ,  $A_{1/2}$ ,  $A_{3/2}$  need to be process-independent. The same argument is applied to the eleven parameters,  $P'$ ,  $\epsilon_a$ ,  $\epsilon_{3/2}$ ,  $\epsilon_T$ ,  $q$ ,  $q_C$ ,  $\phi_a$ ,  $\phi$ ,  $\phi_T$ ,  $\omega$ ,  $\omega_C$ . One should note that the isospin symmetry and the process-independence are closely correlated. It is easy to see that, if the parameters are process-dependent, then the isospin symmetry would be broken,

unless there would exist more complicate relations between these eleven parameters. But this seems violating the basic physics principle: the simple law for complicate phenomena.

There are total twelve parameters to be determined, but we have only eight independent measurements, four sets of branching rates and asymmetries. (We identify the measurement for the mixing induced CP asymmetry  $S_{\pi^0 K_S^0}$  as an independent test for the weak angle  $\beta$  and our model.) It is impossible to completely determine all the parameters. In the next section, the QCDF with three parton corrections is used to calculate the eleven parameters, except of the angle  $\gamma$ , because they are closely related to the strong interactions. Further more, the three phases  $\phi_a, \phi, \phi_T$  are assumed to contain both perturbative and nonperturbative QCD contributions. The perturbative parts  $\hat{\phi}_a, \hat{\phi}, \hat{\phi}_T$ , are calculated by the QCDF formalism and the nonperturbative  $\bar{\phi}_a, \bar{\phi}, \bar{\phi}_T$  determined by fitting to the experimental data. If the factorization scale  $\mu$  for each process are also identified as independent parameters,  $\mu_i, i = 1, \dots, 4$ . Then, there are total eight parameters,  $\phi_a, \bar{\phi}, \phi_T, \gamma$ , and  $\mu_i$ , which can be completely determined by eight measurements. We identify this model as the minimal QCDF model (MQCDF) to distinguish the other similar models, such as the final state interactions [27] or end-point divergences [30].

One should note that the above defined amplitude parameters would be functions of some intrinsic variable,  $x$ , which may or may not depends on processes. In our model based on QCDF, the intrinsic variable is defined as the factorization scale  $\mu$ . This is because the factorization scale is to separate the short distance physics from the long distance one. The scale invariance means that the amplitude would be invariant under different choice of the factorization scale, in principle. However, the above argument is correct if the short distance and the long distance parts of the amplitude are both calculated up to infinite order in  $\alpha_s$  [31]. At finite order accuracy, there always remains some scale dependence in the amplitudes. The choice of the factorization scale is one theoretical degree of freedoms. For different processes, the same amplitude parameter may depend on different factorization scales. From the phenomenological point of view, this is reasonable. The factorization scale denotes the energy scale at which the short distance interactions of the decay process could happen. Different processes have different short distance interactions at the parton level. It is not necessary to require every process to have the same factorization scale. In QCDF, the factorization scale, varying between  $m_b/2$  and  $2m_b$ , with  $m_b$  the  $b$  quark mass, is acceptable. Therefore, it is understood that the above eleven parameters would be functions of  $\mu$ , without explicit mention. One interesting question is that whether the weak angle  $\gamma$  would be process-dependent. As a result, one should not expect to have a universal value of  $\gamma$ . We will later find that  $\gamma$  is process-independent. The further discussions about this point refer to Sec.IV.

If the isospin symmetry is conserved and/or the parameters are process independent, then the scale  $\mu$  would be universal for four processes. On the other hand, different processes would require different factorization scales,  $\mu \rightarrow \mu_i$ . Whether the isospin symmetry is conserved or broken will be studied latter. Further more, the relation between the isospin symmetry and the question whether the parameters are process-dependent or not would be explored, too.

## B. Branching Ratios And Direct CP Asymmetries

In order to explicitly explore how the puzzle would happen, every term is remained in the following expressions without applying any approximation. Using these amplitude parameters, the branching ratios are expressed as

$$Br(\pi^- K^0) = \Gamma_{B^-} P'^2 [1 + 2\epsilon_a \cos(\phi_a) \cos(\gamma) + \epsilon_a^2], \quad (7)$$

$$\begin{aligned} Br(\pi^0 K^-) = & \frac{1}{2} \Gamma_{B^-} P'^2 [1 + \epsilon_{3/2}^2 + \epsilon_a^2 + \epsilon_{3/2}^2 q^2 \\ & + 2\epsilon_a \cos(\phi_a) \cos(\gamma) - 2\epsilon_{3/2} \cos(\phi) \cos(\gamma) \\ & + 2\epsilon_{3/2} q \cos(\omega + \phi) - 2\epsilon_{3/2} \epsilon_a \cos(\phi - \phi_a) \\ & - 2\epsilon_{3/2}^2 q \cos(\omega) \cos(\gamma) \\ & + 2\epsilon_{3/2} \epsilon_a q \cos(\omega + \phi - \phi_a) \cos(\gamma)], \end{aligned} \quad (8)$$

$$\begin{aligned} Br(\pi^+ K^-) = & \Gamma_{B^0} P'^2 [1 + \epsilon_T^2 + \epsilon_a^2 + \epsilon_T^2 q^2 \\ & + 2\epsilon_a \cos(\phi_a) \cos(\gamma) - 2\epsilon_T \cos(\phi_T) \cos(\gamma) \\ & + 2\epsilon_T q \cos(\omega + \phi_T) - 2\epsilon_T \epsilon_a \cos(\phi_T - \phi_a) \\ & - 2\epsilon_T^2 q \cos(\omega) \cos(\gamma) \\ & + 2\epsilon_T \epsilon_a q \cos(\omega + \phi_T - \phi_a) \cos(\gamma)], \end{aligned} \quad (9)$$

$$\begin{aligned} Br(\pi^0 K^0) = & \frac{1}{2} \Gamma_{B^0} P'^2 [1 + \epsilon_a^2 + \epsilon_{3/2}^2 \\ & + \epsilon_{3/2}^2 q^2 + \epsilon_T^2 + \epsilon_T^2 q^2 \\ & + 2\epsilon_a \cos(\phi_a) \cos(\gamma) - 2\epsilon_{3/2} \cos(\phi) \cos(\gamma) \\ & - 2\epsilon_T \cos(\phi_T) \cos(\gamma) + 2\epsilon_{3/2} q \cos(\omega + \phi) \\ & - 2\epsilon_{3/2} \epsilon_a \cos(\phi - \phi_a) + 2\epsilon_T q \cos(\omega_C + \phi_T) \\ & - 2\epsilon_T \epsilon_a \cos(\phi_T - \phi_a) - 2\epsilon_{3/2}^2 q \cos(\omega) \cos(\gamma) \\ & - 2\epsilon_T^2 q \cos(\omega_C) \cos(\gamma) \\ & + 2\epsilon_{3/2} \epsilon_a q \cos(\omega + \phi - \phi_a) \cos(\gamma) \\ & + 2\epsilon_T \epsilon_a q \cos(\omega_C + \phi_T - \phi_a) \cos(\gamma)], \end{aligned} \quad (10)$$

and the direct CP asymmetries written as

$$A_{CP}(\pi^- K^0) = N(\pi^- K^0) \epsilon_a \sin(\phi_a) \sin(\gamma), \quad (11)$$

$$A_{CP}(\pi^0 K^-) = N(\pi^0 K^-) \sin(\gamma) [\epsilon_a \sin(\phi_a) - \epsilon_{3/2} \sin(\phi) + \epsilon_{3/2}^2 q \sin(\omega) - \epsilon_a \epsilon_{3/2} q \sin(-\phi_a + \phi + \omega)], \quad (12)$$

$$A_{CP}(\pi^+ K^-) = N(\pi^+ K^-) \sin(\gamma) [\epsilon_a \sin(\phi_a) - \epsilon_T \sin(\phi_T) + \epsilon_T^2 q_C \sin(\omega_C) - \epsilon_a \epsilon_T q \sin(-\phi_a + \phi_T + \omega_C)], \quad (13)$$

$$A_{CP}(\pi^0 K^0) = N(\pi^0 K^0) \sin(\gamma) [\epsilon_a \sin(\phi_a) + (\epsilon_{3/2} \sin(\phi) - \epsilon_T \sin(\phi_T)) + (\epsilon_{3/2}^2 q \sin(\omega) + \epsilon_T^2 q_C \sin(\omega_C)) + \epsilon_a (\epsilon_{3/2} q \sin(-\phi_a + \phi + \omega) - \epsilon_T q_C \sin(-\phi_a + \phi_T + \omega_C)) - \epsilon_{3/2} (\epsilon_T q \sin(\phi - \phi_T + \omega) + \epsilon_T q_C \sin(-\phi + \phi_T + \omega_C))], \quad (14)$$

where

$$N(\pi K) = \frac{2P'^2}{Br(\pi K)} \Gamma_B.$$

The branching ratios are calculated according to

$$Br(B \rightarrow \pi K) = \frac{1}{2} \Gamma(|A(B \rightarrow \pi K)|^2 + |A(\bar{B} \rightarrow \pi K)|^2)$$

where

$$\Gamma_B = \frac{\tau_B}{16\pi m_B}.$$

According to the particle data group (PDG) definition [4], the CP asymmetry is defined by

$$A_{CP} = \frac{Br(\bar{B} \rightarrow \bar{f}) - Br(B \rightarrow f)}{Br(\bar{B} \rightarrow \bar{f}) + Br(B \rightarrow f)}.$$

Three ratios,

$$R = \frac{Br(\pi^+ K^-) + Br(\pi^0 K^0)}{Br(\pi^- K^0) + Br(\pi^0 K^-)} \frac{\Gamma_{B^-}}{\Gamma_{B^0}}, \quad (15)$$

$$R_c = 2 \left[ \frac{Br(B^- \rightarrow \pi^0 K^-)}{Br(B^- \rightarrow \pi^- \bar{K}^0)} \right], \quad (16)$$

$$R_n = \frac{1}{2} \left[ \frac{Br(\bar{B}^0 \rightarrow \pi^- K^+)}{Br(\bar{B}^0 \rightarrow \pi^0 K^0)} \right], \quad (17)$$

have been widely used in literature as tests for the SM. The comparisons between the theoretical predictions and experimental data of these quantities are left to Sec.V.

### III. CALCULATIONS

At the factorization scale  $\mu \sim m_b$  (the bottom  $b$  quark mass), the effective weak Hamiltonian for  $B \rightarrow \pi K$  decays is given by [43, 44]

$$H_{eff} = \frac{G_F}{\sqrt{2}} \sum_{p=u,c} \lambda_p [C_1(\mu) Q_1^p(\mu) + C_2(\mu) Q_2^p(\mu) + \sum_{i=3,\dots,10} C_i(\mu) Q_i(\mu) + C_{7\gamma}(\mu) Q_{7\gamma}(\mu) + C_{8G}(\mu) Q_{8G}(\mu)] + h.c. \quad (18)$$

where  $\lambda_p = V_{ps}^* V_{pb}$  is the product of CKM matrix elements. The local  $\Delta B = 1$  four quark operators  $Q_i$  are defined as

$$Q_1^p = (\bar{s}_\alpha p_\alpha)_{(V-A)} (\bar{p}_\beta b_\beta)_{(V-A)}, \quad (19)$$

$$Q_2^p = (\bar{s}_\alpha p_\beta)_{(V-A)} (\bar{p}_\beta b_\alpha)_{(V-A)},$$

$$Q_{3,5} = (\bar{s}_\beta b_\beta)_{(V-A)} \sum_{q'} (\bar{q}'_\alpha q'_\alpha)_{(V \mp A)},$$

$$Q_{4,6} = (\bar{s}_\beta b_\alpha)_{(V-A)} \sum_{q'} (\bar{q}'_\alpha q'_\beta)_{(V \mp A)},$$

$$Q_{7,9} = \frac{3}{2} (\bar{s}_\beta b_\beta)_{(V-A)} \sum_{q'} e_{q'} (\bar{q}'_\alpha q'_\alpha)_{(V \pm A)},$$

$$Q_{8,10} = \frac{3}{2} (\bar{s}_\beta b_\alpha)_{(V-A)} \sum_{q'} e_{q'} (\bar{q}'_\alpha q'_\beta)_{(V \mp A)},$$

$$Q_{7\gamma} = -\frac{e}{8\pi^2} (\bar{q} \sigma^{\mu\nu} (1 + \gamma_5) b) F_{\mu\nu},$$

$$Q_{8G} = -\frac{g}{8\pi^2} m_b (\bar{q} \sigma^{\mu\nu} (1 + \gamma_5) b) G_{\mu\nu},$$

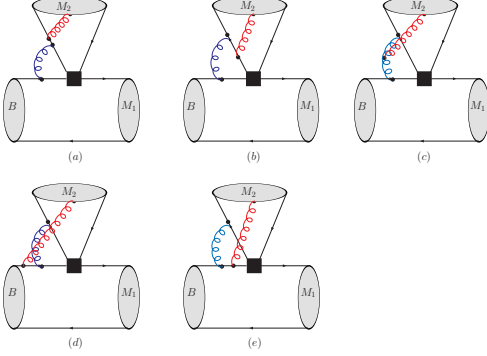
where  $q' \in \{u, d, s, c, b\}$ ,  $\alpha$  and  $\beta$  mean color indices, and  $e_{q'} = 2/3(-1/3)$  for  $u(d)$  type quarks. The Wilson coefficients  $C_i(\mu)$  collect the radiative contributions between  $\mu$  and  $M_W$  up to next-to-leading order (NLO) in  $\alpha_s$ . The renormalization scheme is chosen as the minimal-subtraction ( $\overline{MS}$ ) with  $\Lambda_{\overline{MS}}^{(5)} = 0.225$  GeV. The  $C_i$  are calculated by the naive dimensional regularization (NDR).

Assume the naive factorization  $\langle \pi K | Q_i(0) | B \rangle = \langle \pi | \bar{q}_1 \Gamma_{i,\mu} b | B \rangle \langle K | \bar{q}_2 \Gamma_i^\mu q_3 | 0 \rangle$  or  $\langle K | \bar{q}_1 \Gamma_{i,\mu} b | B \rangle \langle \pi | \bar{q}_2 \Gamma_i^\mu q_3 | 0 \rangle$ , with  $\Gamma_{u,i} \otimes \Gamma_i^\mu = \gamma_\mu (1 - \gamma_5) \otimes \gamma^\mu (1 \pm \gamma_5)$ , and include possible one loop radiative corrections to the factorized terms, the hadronic matrix element  $\langle \pi K | Q_i(0) | B \rangle$  could be expressed in the following factorized form, up-to the twist-3 and NLO in  $\alpha_s$ ,

$$\begin{aligned} \langle \pi K | Q_i(0) | B \rangle &= F_0^{B\pi}(0) \int_0^1 du \text{Tr}[T_{i,K}^I(u) \phi^K(u)] \\ &+ F_0^{BK}(0) \int_0^1 du \text{Tr}[T_{i,\pi}^I(u) \phi^\pi(u)] \\ &+ \int_0^\infty d\xi \int_0^1 du \int_0^1 dv \text{Tr}[\phi^B(\xi) T_{i,B\pi K}^{II}(\xi, u, v) \phi^\pi(u) \phi^K(v)], \end{aligned} \quad (20)$$

where Tr means the trace taken over the spin indices and the integrals are made over the momentum fractions  $u, v, \xi$ . The hard scattering kernels,  $T^{I,II}$ , describe the

Figure 1. Three parton one loop diagrams for the vertex corrections of  $T^I$  are shown. The red gluon line means the gluonic parton  $g$  of the three parton  $|q\bar{q}g\rangle$  state of the external  $M_2$  meson state  $|M_2\rangle$ . The blue gluon line means the radiative loop gluons. The black box means the effective four quark operator. The other similar diagrams with the gluonic parton line connected to other external or internal parton lines to the vertex or penguin radiative loop corrections may also contribute. Similar three parton one loop diagrams for the  $T^{II}$  are not shown here.



short distance interactions between partons of the external initial and final state mesons. The kernel  $T^I$  contains tree (T), vertex (V), and penguin (P) contributions. The kernel  $T^{II}$  contains hard spectator (HS). The hard scattering kernels, in principle, can be completely calculated by perturbative theories. The transition form factors,  $F_0^{B\pi}$  and  $F_0^{BK}$ , and the meson spin distribution amplitudes  $\phi^B$ ,  $\phi^\pi$ ,  $\phi^K$  encode the long distance interactions of the quarks and gluons. The validity of the factorization formula is explained below.

The factorization at leading twist order has been well-known [11, 30]. In the following, let's concentrate on the twist-3 level.

At the twist-3 two parton order, the hard spectator terms may contain end-point divergences in the form

$$X_H = \int_0^1 du \frac{\phi_p(u)}{u},$$

if the twist-3 two parton pseudo-scalar distribution amplitude  $\phi_p$  is a constant [11, 30]. This viewpoint of a constant  $\phi_p$  has been widely employed in literature. However, this is not the correct fact, because a constant  $\phi_p$  is determined by the equation of motion (EOM) at the chiral symmetry breaking scale  $\mu_c \sim 1$  GeV. The partons involving in the hard scattering kernels  $T^{II}$  would have energies about the energetic scale  $\mu_E \sim m_b \gg \mu_c$ . The correct EOM of  $\phi_p$  would be taken at the energetic scale  $\mu_E$  instead of  $\mu_c$ . As a result,  $\phi_p$  becomes equal to  $\phi_\sigma$  and not a constant. The above mentioned end-point divergences in the hard spectator terms would vanish [40].

There also exist end-point divergences from the annihilation terms in the form

$$X_A = \int_0^1 du \frac{\phi_P(u)}{u(u-\xi)},$$

even for the twist-2 pseudo-scalar distribution amplitude  $\phi_P$  [11, 30]. The regularization method is not to neglect the momentum fraction factor  $\xi$  from the spectator lines of the  $B$  meson. It can be shown that the regularized result is equivalent to include the twist-4 contributions [45]. As a result, the annihilation terms up to twist-3 are also factorizable. The annihilation terms are not included in the above factorization formula and will be neglected in later calculations.

According to the study by Yeh [45], there are five types of different ways as shown in Fig 1 that the three parton state  $|q\bar{q}g\rangle$  of the emitted final state meson  $M = \pi, K$  can contribute at one loop level. The three parton state from the  $B$  meson needs not be considered, because only soft spectator gluonic partons can involve and their contributions are power suppressed by  $O(1/m_B^2)$ . By power counting [40], it is easy to see that only contributions from Fig. 1(a) are leading at twist-3 order (i.e., suppressed by  $O(1/m_B)$ ) and the other five types of contributions are at least of twist-4 (i.e., suppressed by  $O(1/m_B^2)$  than the leading twist-2 term). Considering only contributions from Fig. 1(a), the meson spin distribution amplitude  $\phi^M(u)$  for  $M = \pi, K$  has the following spin representation [40]

$$\begin{aligned} \phi^M(u) &= \int_0^\infty \frac{d\lambda}{2\pi} e^{-iu\lambda} \langle M | \bar{q}_a(0) q_b(\frac{\lambda}{E}n) | 0 \rangle \\ &+ \int_0^\infty \frac{d\lambda}{2\pi} \int_0^\infty \frac{d\eta}{2\pi} e^{-i\alpha\lambda} e^{-i\eta\beta} \langle M_2 | \bar{q}_a(0) i g A(\frac{\eta}{E}n) q_b(\frac{\lambda}{E}n) | 0 \rangle \\ &= -\frac{if_M}{4N_c} \left[ \gamma_5 \not{A} \phi_P(u) + \mu_\chi \left( \gamma_5 \phi_p(u) - \frac{1}{2} \epsilon_\perp \cdot \sigma \phi_\sigma(u) \right. \right. \\ &\quad \left. \left. + 2\gamma_5 \delta(u - \alpha - \beta) \int_0^1 d\alpha \int_0^{(1-\alpha)} d\beta \frac{\phi_{3p}(\alpha, \beta)}{\alpha\beta} \right) \right], \end{aligned} \quad (21)$$

where  $f_M$  is the decay constant and  $\mu_\chi^M = m_M^2/(m_{q_a} + m_{q_b})$  the chiral enhanced factor.  $\phi_P$  is the twist-2 pseudo-scalar distribution function and  $\phi_p$  and  $\phi_\sigma$  are twist-3 two parton pseudo-scalar and pseudo-tensor distribution functions. The three parton distribution function  $\phi_{3p}$  is defined by

$$\begin{aligned} &\int_0^\infty \frac{d\lambda}{2\pi} \int_0^\infty \frac{d\eta}{2\pi} e^{-i\alpha\lambda} e^{-i\eta\beta} \\ &\langle M_2 | \bar{q}(0) \gamma_5 \sigma^{\alpha\beta} g G^{\mu\nu}(\frac{\eta}{E}n) q(\frac{\lambda}{E}n) | 0 \rangle \\ &= -if_M \mu_\chi P^{\alpha\beta\mu\nu}(q) \phi_{3p}(\alpha, \beta) \end{aligned} \quad (22)$$

and has a parametrization

$$\phi_{3p}(\alpha, \beta) = 360\eta\alpha\beta^2(1 - \alpha - \beta)(1 + \frac{1}{2}\omega(7\beta - 3)) \quad (23)$$

with  $\eta = 0.015$  and  $\omega = -3$ . This representation of the spin distribution  $\phi^M$  is written according to the following facts:

- The effective spin structure and the nontrivial integrals of  $\phi_{3p}$  can be derived from the tree level

Feynman diagrams similar to the Fig.1(a), in which the radiative gluon is absorbed by the vertex. The detailed derivations refer to [40]. When the three parton one loop Feynman diagrams as depicted in Fig.1(a) are considered, it can be easily derived that the same spin structure is also applicable. Effectively, one may regard the three parton in this scenario as a pseudo-scalar two parton term. This shows a very convenient way to calculate the three parton one loop corrections by simply referring to those one loop calculations of  $\phi_p$  [45].

- It can be easily shown that the energetic EOM  $\phi_p = \phi_\sigma$  would not change if  $\phi_{3p}$  is considered. This is because the spin projector  $P^{\alpha\beta\mu\nu}(q)$  vanishes at the energetic EOM condition. It implies that  $\phi_p$  and  $\phi_\sigma$  decouple from  $\phi_{3p}$  at the energetic limit  $E \gg \Lambda_{QCD}$ .

Combining the above two facts, it can be shown that the one loop corrections of  $\phi_{3p}$  are factorizable according to the analysis for the factorizability of the one loop corrections of  $\phi_p$  given in [45]. The complete analysis of the above arguments will be present elsewhere. The  $B$  meson spin distribution amplitude is given by [45]

$$\begin{aligned}\phi^B(\xi) &= \int_0^\infty \frac{d\lambda}{2\pi} e^{-i\xi\lambda} \langle 0 | \bar{q}(0) b(\frac{\lambda}{E} n) | B \rangle \\ &= \frac{if_B}{4N_c} [(\not{P}_B + m_B) \gamma_5 \phi_B(\xi)] .\end{aligned}$$

For numeric calculations, we employ the following models for  $\phi_B(\xi)$ ,  $\phi_P(u)$ ,  $\phi_p(u)$

$$\begin{aligned}\phi_P(u) &= \phi_p(u) = 6u(1-u) , \\ \phi_B(\xi) &= \frac{N_B \xi^2 \bar{\xi}^2}{[\xi^2 + \epsilon_B \bar{\xi}]^2} ,\end{aligned}$$

with  $N_B = 0.133$ ,  $\epsilon_B = 0.005$  for  $\lambda_B = 350$  MeV.  $N_B$  and  $\epsilon_B$  are determined by the moments

$$\int_0^1 d\xi \phi_B(\xi) = 1, \quad \int_0^1 d\xi \frac{\phi_B(\xi)}{\xi} = \frac{m_B}{\lambda_B} ,$$

where the errors are controlled within 1%. Since the scale dependent correctional terms of the meson distribution amplitudes start at NNLO  $O(\alpha_s^2)$ , they could be neglected at NLO calculations.

Summarizing the above analysis, it shows that the factorization formula of QCDF given in Eq.(20) is valid up to complete twist-3 power corrections and NLO in  $\alpha_s$ . Due to their smallness as compared with the other types of contributions, we will completely neglect the annihilation terms. This makes our later explanations for the puzzle completely different from most literature based on QCDF, in which the annihilation electro-weak penguin terms would be important [11, 30].

In the following, the tree, vertex, penguin, and hard spectator contributions are collected as  $a_i(\pi K)$  for each

$Q_i$  as given below

$$\begin{aligned}a_i^p(\pi K, \mu) &= (C_i(\mu) + \frac{C_{i\pm 1}(\mu)}{N_c}) N_i(K) \\ &+ \frac{C_{i\pm 1}(\mu)}{N_c} \frac{\alpha_s(\mu) C_F}{4\pi} [V_i^{(2)}(K) + V_i^{(3)}(K)] \\ &+ (4\pi\alpha_s(\mu) C_F) \frac{C_{i\pm 1}(\mu)}{N_c^2} [H_i^{(2)}(\pi K) + H_i^{(3)}(\pi K)] \\ &+ P_i^{p(2)}(K, \mu) + P_i^{p(3)}(K, \mu) .\end{aligned}\tag{24}$$

The expressions for the tree  $N_i(K)$ , the two parton vertex  $V_i^{(2)}(K)$ , the two parton hard spectator  $H_i^{(2)}(\pi K)$ , and the two parton penguin  $P_i^{p(2)}(K)$  are referred to [11, 45]. Here, we only present the three parton vertex  $V_{6,8}^{(3)}(K)$ , the three parton hard spectator  $H_i^{(3)}(\pi K)$ , and the three parton penguin  $P_{6,8}^{p(3)}(K, \mu)$  as follows

$$\begin{aligned}V_{6,8}^{(3)}(K) &= 2 \int_0^1 du \int_0^{(1-u)} dv \left[ \frac{\phi_{3p}(u, v)(-6 + h^{(3)}(u, v))}{uv} \right] ,\end{aligned}\tag{25}$$

where the kernel is

$$\begin{aligned}h^{(3)}(u, v) &= 2 [\text{Li}_2(x) + \frac{1}{2}(\ln \bar{x})^2 - (x \leftrightarrow (1-x))]_{x=u+v} .\end{aligned}\tag{26}$$

The penguin functions  $P_{6,8}^{p(3)}(K, \mu)$  are given by

$$\begin{aligned}P_6^{p(3)}(K, \mu) &= \frac{\alpha_s(\mu) C_F}{4\pi N_c} \left\{ C_1(\mu) \left[ \left( \frac{4}{3} \ln \frac{m_b}{\mu} + \frac{2}{3} \right) A_G - G_K^{(3)}(s_p) \right] \right. \\ &+ C_3(\mu) \left[ 2 \left( \frac{4}{3} \ln \frac{m_b}{\mu} + \frac{2}{3} \right) A_G - G_K^{(3)}(0) - G_K^{(3)}(1) \right] \\ &+ (C_4(\mu) + C_6(\mu)) \\ &\left. \left[ \frac{4}{3} n_f \left( \ln \frac{m_b}{\mu} \right) A_G - (n_f - 2) G_K^{(3)}(0) - G_K^{(3)}(s_c) - G_K^{(3)}(1) \right] \right. \\ &\left. - 4C_{8g}^{\text{eff}} \int_0^1 du \int_0^{(1-u)} dv \frac{\phi_{3p}(u, v)}{uv} \right\} ,\end{aligned}\tag{27}$$

$$\begin{aligned}P_8^{p(3)}(\mu) &= \frac{\alpha}{9\pi N_c} \{ (C_1(\mu) + N_c C_2(\mu)) \\ &\left[ \frac{4}{3} A_G \ln \frac{m_b}{\mu} + \frac{2}{3} A_G - G_K^{(3)}(s_p) \right] \\ &- 6C_{7\gamma}^{\text{eff}} \int_0^1 du \int_0^{(1-u)} dv \frac{\phi_{3p}(u, v)}{uv} \} ,\end{aligned}\tag{28}$$

where  $n_f = 5$  denotes the number of the flavors.

The functions  $G_K^{(3)}(s_p)$  is defined as

$$\hat{G}_K^{(3)}(s_c) = 2 \int_0^1 du \int_0^{(1-u)} dv \frac{\phi_{3p}(u, v)}{uv} G(s - i\epsilon, 1 - x)|_{x=u+v},$$

$$G(s, u) = -4 \int_0^1 dx x(1 - x) \ln[s - x(1 - x)u].$$

By substituting  $s_c = 0$ ,  $m_c^2/m_b^2$ , 1,  $G_K(s_p)$  and  $\hat{G}_K(s_p)$  are calculated ( $m_c^2/m_b^2 = 0.09$ ) for later numerical analysis

$$\begin{aligned}\hat{G}_K^{(3)}(0) &= 0.81 - i1.23, \\ \hat{G}_K^{(3)}(s_c) &= 1.26 - i0.94, \\ \hat{G}_K^{(3)}(1) &= 0.059.\end{aligned}$$

The effective Wilson coefficients  $C_{7\gamma}^{\text{eff}}$  and  $C_{8g}^{\text{eff}}$  are calculated at their leading order in  $\alpha_s$  to be constants

$$\begin{aligned}C_{7\gamma}^{\text{eff}} &= -0.32, \\ C_{8g}^{\text{eff}} &= -0.15.\end{aligned}$$

The hard spectator functions  $H_i^{(3)}(\pi K)$  are, for  $i = 1 - 5, 7, 9, 10$ ,

$$\begin{aligned}H_i^{(3)}(\pi K) &= 2 \frac{B_{\pi K}}{A_{\pi K}} m_B r_\chi^\pi(\mu_h) \int_0^1 d\xi \frac{\phi_B(\xi)}{\xi} \int_0^1 d\alpha \int_0^{(1-\alpha)} d\beta \int_0^1 du \\ &\times \left[ \frac{\phi_{3p}(\alpha, \beta) \phi_P(u)}{(\alpha + \beta)\alpha\beta(\bar{u} - \xi)} \right],\end{aligned}$$

where

$$B_{\pi K} = i \frac{G_F}{\sqrt{2}} f_B f_K f_\pi$$

and  $H_{6,8}^{(2,3)}(\pi K) = 0$ . The scale in  $r_\chi^\pi(\mu_h)$  is assumed as  $\mu_h = \sqrt{\Lambda_h \mu}$  and  $\Lambda_h = 0.5$  GeV.

According to the QCD factorization formula Eq.(1), we obtain the expressions for the amplitudes [11, 30, 45]

$$\begin{aligned}A(\pi^- \bar{K}^0) &= \lambda_p A_{\pi K} \left[ \left( a_4^p - \frac{1}{2} a_{10}^p \right) \right. \\ &\quad \left. + r_\chi^K \left( a_6^p - \frac{1}{2} a_8^p \right) \right],\end{aligned}\quad (29)$$

$$\begin{aligned}-\sqrt{2} A(\pi^0 K^-) &= A_{\pi K} [\lambda_u a_1 + \lambda_p (a_4^p + a_{10}^p) \\ &\quad + \lambda_p r_\chi^K (a_6^p + a_8^p)] \\ &\quad + A_{K\pi} \left[ \lambda_u a_2 + \lambda_p \frac{3}{2} (-a_7 + a_9) \right],\end{aligned}\quad (30)$$

$$\begin{aligned}-A(\pi^+ K^-) &= A_{\pi K} [\lambda_u a_1 + \lambda_p (a_4^p + a_{10}^p) \\ &\quad + \lambda_p r_\chi^K (a_6^p + a_8^p)],\end{aligned}\quad (31)$$

$$\begin{aligned}\sqrt{2} A(\pi^0 \bar{K}^0) &= \lambda_p A_{\pi K} \left[ \left( a_4^p - \frac{1}{2} a_{10}^p \right) \right. \\ &\quad \left. + r_\chi^K \left( a_6^p - \frac{1}{2} a_8^p \right) \right] \\ &\quad - A_{K\pi} \left[ \lambda_u a_2 + \lambda_p \frac{3}{2} (-a_7 + a_9) \right],\end{aligned}\quad (32)$$

where the  $\mu$  dependence of  $a_i$  is implicitly understood. We have defined the following factors

$$\begin{aligned}A_{\pi K} &= i \frac{G_F}{\sqrt{2}} (m_B^2 - m_\pi^2) F_0^{B\pi}(m_K^2) f_K, \\ A_{K\pi} &= i \frac{G_F}{\sqrt{2}} (m_B^2 - m_K^2) F_0^{BK}(m_\pi^2) f_\pi,\end{aligned}$$

$$\begin{aligned}r_\chi^K &= \frac{2m_K^2}{m_b(m_q + m_s)} (1 + A_G), \quad \lambda_u = \lambda_c \tan^2 \theta_c R_b e^{-i\gamma}, \\ \tan^2 \theta_c &= \frac{\lambda^2}{1 - \lambda^2}, \quad R_b = \frac{1 - \lambda^2/2}{\lambda} \left| \frac{V_{ub}}{V_{cb}} \right|, \quad \lambda = |V_{us}|.\end{aligned}$$

The three parton tree factor  $A_G$  comes from the integration [40]

$$A_G = 2 \int_0^1 d\alpha \int_0^{(1-\alpha)} d\beta \frac{\phi_{3p}(\alpha, \beta)}{\alpha\beta}.$$

By comparing expressions given in Eq(1) and Eq.(29), the perturbative parts of the amplitude parameters are calculated to be [30]

$$P' = \lambda_c A_{\pi K} \left[ \left( a_4^c - \frac{1}{2} a_{10}^c \right) + r_\chi^K \left( a_6^c - \frac{1}{2} a_8^c \right) \right], \quad (33)$$

$$\epsilon_a e^{i\hat{\phi}_a} = \epsilon_{KM} \frac{(a_4^u - \frac{1}{2} a_{10}^u) + r_\chi^K (a_6^u - \frac{1}{2} a_8^u)}{(a_4^c - \frac{1}{2} a_{10}^c) + r_\chi^K (a_6^c - \frac{1}{2} a_8^c)}, \quad (34)$$

$$\begin{aligned}\epsilon_{3/2} e^{i\hat{\phi}} &= -\epsilon_{KM} \\ &\quad \frac{a_1 + R_{\pi K} a_2 + \frac{3}{2} (a_{10}^u + r_\chi^K a_8^u + R_{\pi K} (a_9 - a_7))}{(a_4^c - \frac{1}{2} a_{10}^c) + r_\chi^K (a_6^c - \frac{1}{2} a_8^c)},\end{aligned}\quad (35)$$

$$\epsilon_T e^{i\hat{\phi}_T} = -\epsilon_{KM} \frac{a_1 + \frac{3}{2} (a_{10}^u + r_\chi^K a_8^u)}{(a_4^c - \frac{1}{2} a_{10}^c) + r_\chi^K (a_6^c - \frac{1}{2} a_8^c)}, \quad (36)$$

$$q e^{i\omega} = -\frac{3}{2\epsilon_{KM}} \quad (37)$$

$$\begin{aligned}q_C e^{i\omega_C} &= -\frac{3}{2\epsilon_{KM}} \frac{a_{10}^c + r_\chi^K a_8^c + R_{\pi K} (a_9 - a_7)}{a_1 + R_{\pi K} a_2 + \frac{3}{2} (a_{10}^u + r_\chi^K a_8^u + R_{\pi K} (a_9 - a_7))}, \\ &\quad \frac{a_{10}^c + r_\chi^K a_8^c}{a_1 + \frac{3}{2} (a_{10}^u + r_\chi^K a_8^u)},\end{aligned}\quad (38)$$

where the notations

$$R_{\pi K} = \frac{A_{K\pi}}{A_{\pi K}}, \quad \epsilon_{KM} = \frac{|\lambda_u|}{|\lambda_c|} \simeq \frac{\lambda^2}{2},$$

are defined.

The parameters would be process dependent due to the scale  $\mu$  of the  $a_i$ . The scale  $\mu$  could be different from the assumed  $\mu = m_b$  and also depends on the process. These complicate relations are represented by the  $\mu_i$  with  $i$  as an index for different processes. Therefore, these parameters are interpreted as functions of  $\mu_i$  and calculated through the above equations Eqs.(33-38). In this work, we will assume that the hadronic terms  $P$ ,  $\epsilon_a$ ,  $\epsilon_{3/2}$ ,  $\epsilon_T$ ,  $q$  and  $q_C$  and the two strong phases  $\omega$  and  $\omega_C$  are pure



perturbative and allow the strong phases  $\phi_a$ ,  $\phi$ , and  $\phi_T$  contain both perturbative  $\hat{\phi}_a$ ,  $\hat{\phi}$ , and  $\hat{\phi}_T$  and nonperturbative parts  $\bar{\phi}_a$ ,  $\bar{\phi}$ , and  $\bar{\phi}_T$ :

$$\begin{aligned}\phi_a &= \hat{\phi}_a + \bar{\phi}_a, \\ \phi &= \hat{\phi} + \bar{\phi}, \\ \phi_T &= \hat{\phi}_T + \bar{\phi}_T.\end{aligned}$$

This is because only  $\phi_a$ ,  $\phi$ , and  $\phi_T$  can directly involve in the direct CP asymmetries. These phase factors  $\bar{\phi}_a$ ,  $\bar{\phi}$ , and  $\bar{\phi}_T$  could be of SM or NP. If they are of SM, then they are pure strong phases. But, they could be from any NP model. We leave this point as an open question.

#### IV. ANALYSIS

In order to determine the four parameters,  $\gamma$ ,  $\bar{\phi}_a$ ,  $\bar{\phi}$ , and  $\bar{\phi}_T$ , introduced in the above, we employ the following fitting procedure by using the eight measurements of four branching ratios and four direct CP asymmetries. The input data given in Table I are used to calculate the amplitude parameters given in Eqs.(33-38), which are then substituted into the Eqs.(7-14). The data are separated into four sets, one set for one process. Each set contains one branching ratio and one asymmetry: Set-1:  $Br(\pi^- \bar{K}^0)$  and  $A_{CP}(\pi^- \bar{K}_s^0)$ ; Set-2:  $Br(\pi^0 K^-)$  and  $A_{CP}(\pi^0 K^-)$ ; Set-3:  $Br(\pi^+ K^-)$  and  $A_{CP}(\pi^+ K^-)$ ; Set-4:  $Br(\pi^0 \bar{K}^0)$  and  $A_{CP}(\pi^0 \bar{K}^0)$ . Their experimental data are present in Table IV, in which only the PDG2016 data [4] are used and the HFAG2016 data [18] are listed for reference. The least square fit method is used. The  $\chi^2$  function is defined as

$$\chi_i^2(\vec{\theta}) = \sum_{j=1}^2 \frac{(O_{ij}^{exp} - O_{ij}^{th}(\vec{\theta}))^2}{\sigma_{ij}^2}, \quad (39)$$

$$\chi_{tot}^2(\vec{\theta}) = \sum_{i=1}^4 \chi_i^2(\vec{\theta}), \quad (40)$$

where  $\chi_i^2$  is the  $\chi^2$  function for the  $i$ -th set of data:  $i = 1$  for  $B^- \rightarrow \pi^- \bar{K}^0$ ,  $i = 2$  for  $B^- \rightarrow \pi^0 K^-$ ,  $i = 3$  for  $\bar{B}^0 \rightarrow \pi^+ K^-$  and  $i = 4$  for  $\bar{B}^0 \rightarrow \pi^0 \bar{K}^0$ . The fitting parameters are  $\vec{\theta} = (\mu_i, i = 1, \dots, 4; \gamma, \bar{\phi}_a, \bar{\phi}, \bar{\phi}_T)$ . The scale variable  $\mu_i$  is defined for  $i$ -th data set. The experimental measurements  $O_{ij}^{exp}$ , the theoretical predictions  $O_{ij}^{th}$ , and the experimental errors  $\sigma_{ij}$  are for the  $j$ -th measurement of the  $i$ -th data set,  $j = 1$  for the branching rate and  $j = 2$  for the asymmetry. For each fitting process, only two measurements and one parameter are used. The degrees of freedom is equal to one, according to the least square fit method. However, the nonlinear functional form of the expressions for the branching ratios and the asymmetries makes the fitting to be a nonlinear least square fit problem. It is not appropriate by using the standard least  $\chi^2$  fit method, in which all the parameters are simultaneously determined by calculating the

best-fit value of the  $\chi^2$  function. To improve the task of fitting, we design the following strategy similar to the Marquardt method [46]. The value of  $\chi^2 = \chi_i^2, \chi_{tot}^2$  for each fitting process is very close to zero,  $\chi^2 \simeq 0$ .

#### A. Fitting Strategy

The following fitting strategy is employed to determine the parameters  $\gamma$ ,  $\bar{\phi}_a, \bar{\phi}, \bar{\phi}_T$  and the scale variables  $\mu_i$ ,  $i = 1, \dots, 4$ .

1. Choose a reference value  $\gamma_{init}$  for the weak angle  $\gamma$ . Here,  $\gamma_{init} = 72.1$  is chosen for the world averaged value  $72.1_{-5.8}^{+5.4}$ [18].
2. Calculate the  $\chi^2$  value for set  $i = 1, \dots, 4$  by varying the factorization scale variable  $\mu_i$  within the range  $m_b/2 \leq \mu_i \leq 2m_b$  to find a least  $\chi_{i,\mu}^2$  at the temporal  $\mu_i^T$ .
3. Calculate the  $\chi^2$  value for data set  $i$  by varying one of the strong phase variables  $\bar{\phi}_a, \bar{\phi}, \bar{\phi}_T$  within the range  $-180^\circ \leq \bar{\phi}_a, \bar{\phi}, \bar{\phi}_T \leq 180^\circ$  with the previous temporal  $\mu_i^T$  to find a least  $\chi_{i,\phi}^2$  at the temporal  $\bar{\phi}_{a,i}^T, \bar{\phi}_i^T, \bar{\phi}_{T,i}^T$ .
4. Repeat procedures 3 and 4 until  $\chi_{i,\mu}^2 = \chi_{i,\phi}^2$  and obtain the fitting values of  $\mu_i, \bar{\phi}_{a,i}, \bar{\phi}_i, \bar{\phi}_{T,i}$ .
5. The fitted values of  $\mu_i, \bar{\phi}_{a,i}, \bar{\phi}_i, \bar{\phi}_{T,i}$  are used to calculate the least  $\chi^2$  for all data by varying  $-180^\circ \leq \gamma \leq 180^\circ$  to find a least  $\chi_{tot}^2$  at  $\gamma_{fit}$ .
6. Use  $\gamma_{fit}$  to repeat procedures 2-6 until the  $\chi_{tot}^2$  reaches a stable least value.
7. Use the criteria  $\chi^2/\sqrt{2\nu} \leq 1$  to set the upper and lower bounds of each parameter.  $\nu$  is the degrees of freedom of the used data points and defined as  $\nu = N - n$  with  $N$  the number of data point and  $n$  the number of the fitting parameters. For the procedures 3 and 4,  $N = 2$  and  $n = 1$  and  $\nu = 1$ . The bounds of  $\gamma_{fit}$  are determined by using  $\chi^2/\sqrt{2\nu} \leq 1$  for  $\nu = N - n = 4$  with  $N = 8$  and  $n = 4$ .

#### B. Fitting Results

The fitted results for  $\mu, \bar{\phi}_a, \bar{\phi}, \bar{\phi}_T$  and  $\gamma$  are listed in the Table.II. The amplitudes parameters calculated at  $\mu_i$  are list in Table.III. For comparison, the amplitudes parameters calculated for  $m_b/2 \leq \mu \leq 2m_b$  with its central value at  $\mu = \mu_0 = m_b$  are also listed (denoted as  $\mu_0$ ) in the same table. The fitted scales  $\mu_i$  are used to calculate the averaged scale  $\mu_{av}$ . (See below explanation for  $\mu_{av}$ .) The predictions of QCDF for branching ratios and asymmetries are calculated at  $m_b/2 \leq \mu \leq 2m_b$  and  $\mu = \mu_{av} \pm \sigma_{av}$ , denoted as Naive and Improved columns present in Table IV. Using the fit data to calculate the

predictions for the branching ratios and asymmetries are given in the Fit column in Table IV, where the first errors are from  $\mu_i$  and the second errors from the phase factors,  $\bar{\phi}_a, \bar{\phi}, \bar{\phi}_T$ .

Comments of the above analysis are given as follows.

- In QCDF, the factorization scale  $\mu$  separates the perturbative physics from the nonperturbative. Priority, it is not possible to guess what scale is appropriate for a process. In the  $B$  decays,  $\mu = m_b$  is a convenient but not absolute choice. Any  $\mu$  within the range  $m_b/2 \leq \mu \leq 2m_b$  is allowable. According to the fitted result, different processes require different factorization scales. This is consistent with the factorization theorem, since choosing  $\mu$  is the degree of freedom of QCDF. Therefore,  $\mu$  is not identified as a fitting parameter.
- The branching ratios are sensitive to the factorization scale  $\mu$ , while the asymmetries are sensitive to the strong phases  $\phi_a, \phi$ , and  $\phi_T$ .
- The predictions for branching ratios with  $m_b/2 \leq \mu \leq 2m_b$  can cover the experimental data within errors.
- The predictions for  $A_{CP}(B^- \rightarrow \pi^- K_s^0)$  and  $A_{CP}(\bar{B}^0 \rightarrow \pi^+ K^-)$  are in opposite sign to the data, and the predictions for  $A_{CP}(B^- \rightarrow \pi^0 K^-)$  and  $A_{CP}(\bar{B}^0 \rightarrow \pi^0 K^0)$  are in the same sign to the data.
- The predictions for four asymmetries have consistent magnitudes with the experimental data.
- The perturbative parts of  $\phi_a, \phi$ , and  $\phi_T$  are in opposite sign to their nonperturbative parts.
- The strong phases  $\phi_a, \phi$ , and  $\phi_T$  are the sums of the perturbative  $\hat{\phi}_a, \hat{\phi}$ , and  $\hat{\phi}_T$  and the nonperturbative parts  $\bar{\phi}_a, \bar{\phi}$ , and  $\bar{\phi}_T$ , respectively. The results show that the data favor a large negative  $\phi_a$  and moderate negative  $\phi$  and moderate positive  $\phi_T$ . Especially,  $\bar{B}^0 \rightarrow \pi^0 K^0$  mode favors  $\phi \lesssim \phi_T$  to compensate  $\epsilon_{3/2} \gtrsim \epsilon_T$ .
- Within experimental errors, the nonperturbative  $\bar{\phi}_a, \bar{\phi}$ , and  $\bar{\phi}_T$  are almost universal. The major uncertainties come from the  $A_{CP}(B^- \rightarrow \pi^- K^0)$  for  $\bar{\phi}_a$  and  $A_{CP}(\bar{B}^0 \rightarrow \pi^0 K^0)$  for  $\bar{\phi}$  and  $\bar{\phi}_T$ . However, the more accurate asymmetries  $A_{CP}(B^- \rightarrow \pi^0 K^-)$  and  $A_{CP}(\bar{B}^0 \rightarrow \pi^+ K^-)$  require  $\bar{\phi}_a, \bar{\phi}$ , and  $\bar{\phi}_T$  being process dependent.
- $\bar{\phi}_a$  is determined by data set 1 and needs specific values for the data sets 2, 3, 4, respectively.
- $\bar{\phi}$  and  $\bar{\phi}_T$  would be equal and determined by data set 4 and they need specific values for the data sets 2 and 3.

- The fitted values of  $\gamma, \mu, \bar{\phi}_a, \bar{\phi}$ , and  $\bar{\phi}_T$  would be different if the initial value  $\gamma_{init}$  is chosen a different value. This is because the sum of  $\gamma$  and any one of  $\bar{\phi}_a, \bar{\phi}$ , and  $\bar{\phi}_T$  remains unchanged in each process. The better parametrization would be  $\Phi_a = \bar{\phi}_a - \gamma$ ,  $\Phi = \bar{\phi} - \gamma$ , and  $\Phi_T = \bar{\phi}_T - \gamma$ . This allows for further exploration of the NP effects. We leave this point as an open question for future studies.
- In order to avoid some complications of analysis, only uncertainties from the scale variables  $\mu$  and  $\mu_i$  are concerned as theoretical errors. The other types of uncertainties, such as those from the input parameters or the end-point divergences, are completely neglected. We hope that this would not lead to any confusion.

## V. DISCUSSIONS

To examine whether the puzzle could be resolved in our approach, we choose the following topics to discuss.

### A. Basic Results

*a. Fitting* Using the input data given in Table I, we calculate the amplitude parameters in Table III for five different factorization scales. The  $\mu_0$  column presents the calculations at the scale  $\mu = 4.2\text{GeV}$  and is refereed as the “Naive” theoretical predictions. The four scale variables  $\mu_i, i = 1, \dots, 4$ , are obtained by fitting to the four data sets, respectively. The  $\mu_{av}$  column presents the calculations at the scale  $\mu = \mu_{av}$  and is refereed as the “Improved” theoretical predictions. The hadronic parameters and strong phases are calculated at these six different scales. The fit of each data set gives  $\chi^2 \simeq 0$  for one degree of freedom ( $\nu = 1$ ). According to the least square method (see e.g. [47]), a very small  $\chi^2 \ll 1$  could mean either (i) our model is valid, or (ii) the experimental errors are too large, or (iii) the data is too good to be true. Since a poor model can only increase  $\chi^2$ , a too-small value of  $\chi^2$  cannot be indicative of a poor model. This implies that our model could be a good model for the data. The fitted results show that (i) the factorization scale variable  $\mu$  is process dependent, (ii) the strong phase variables  $\phi_a, \phi, \phi_T$  are process dependent. As a result, the eleven amplitude parameters are process dependent as shown in Table III. This observation is in contradiction to the usual assumption that these amplitude parameters are process independent. If this founding that the amplitudes parameters are process dependent is true, then the puzzle found by assuming the amplitude parameters to be process independent would be questionable.

*b. Averaged analysis* From Table II, the factorization scales  $\mu_i$  of four processes are averaged as  $\mu_{av} = 4.96 \pm 1.44\text{GeV}$ , where the averaged factorization scale

Table I. Input data for numerical calculations refer to [4].

B meson parameters				
$\tau(B_d^0)(\text{ps})$	$\tau(B^-)(\text{ps})$	$m_{B^\pm}(\text{GeV})$	$m_{B^0}(\text{GeV})$	
1.52	1.64	5.28	5.28	
perturbative parameter				
$\Lambda_{\overline{MS}}^{(5)}(\text{GeV})$	$m_b(\text{GeV})$	$m_c(\text{GeV})$	$m_s(\text{GeV})$	
0.225	4.2	1.3	0.09	
decay constants and form factors				
$f_K(\text{GeV})$	$f_\pi(\text{GeV})$	$f_B(\text{GeV})$	$F_0^{B\pi}(0)$	$F_0^{BK}(0)$
0.16	0.13	0.2	0.28	0.34
CKM matrix elements				
$ V_{ub} $	$ V_{cb} $	$ V_{us} $	$ V_{cd} $	$ V_{cs} $
0.0037	0.042	0.23	0.22	0.97

Table II. Fit data for the four parameters. Factorization scales and nonperturbative parts of three strong phase parameters,  $\bar{\phi}_a$ ,  $\bar{\phi}$ , and  $\bar{\phi}_T$  are determined by a least  $\chi^2$  fit method. The fitting strategy is described in the text. The upper and lower bounds of the parameters are determined by  $\chi^2 \leq \sqrt{\nu}$  with  $\nu$  the number of degrees of freedom. The fit determines the weak angle  $\gamma = (72.1_{-5.8}^{+5.7})^\circ$ .

decay modes	$\mu(\text{GeV})$	$\bar{\phi}_a(\text{deg})$	$\bar{\phi}(\text{deg})$	$\bar{\phi}_T(\text{deg})$
$B^- \rightarrow \pi^- \bar{K}^0$	$4.55_{-0.25}^{+0.28}$	$-50_{-56}^{+32}$	NA	NA
$B^- \rightarrow \pi^0 K^-$	$5.25_{-0.37}^{+0.45}$	-50	$3.1_{-3.7}^{+3.6}$	NA
$\bar{B}^0 \rightarrow \pi^+ K^-$	$5.6_{-0.26}^{+0.28}$	-115.1	NA	$16.3 \pm 1.4$
$\bar{B}^0 \rightarrow \pi^0 K^0$	$4.40_{-0.33}^{+0.35}$	-92	$23_{-40.6}^{+29.9}$	$23_{-40.6}^{+29.9}$

$\mu_{av} \pm \sigma_{av}$  is calculated by means of the weighted mean method

$$\mu_{av} = \frac{\sum_i \sigma_i \mu_i}{\sum_i \sigma_i}, \quad \sigma_{av} = \left( \frac{1}{\sum_i \sigma_i^2} \right)^{1/2}.$$

The  $\mu_{av}$  denotes the specific energy scale relevant to the  $B \rightarrow \pi K$  decays. For distinguishing, we call the parameters calculated by  $\mu_0 = m_b$  as the ‘‘Naive’’ predictions and those calculated at  $\mu_{av}$  as the ‘‘Improved’’ predictions. The uncertainties of  $\mu_{av}$  come from the experimental data and those of  $\mu_0$  from the naive assumption of QCDF. The  $\mu_{av}$  is more appropriate than  $\mu_0$  for  $B \rightarrow \pi K$  decays from the predictions given in Table IV, in which the Improved are better than the Naive as compared with the corresponding data. The amplitude parameters calculated at  $\mu_{av} \pm \sigma_{av}$  are present in the column  $\mu_{av}$  of Table III.

*c. Three Parton Effects* For comparison, the amplitude parameters with twist-3 three parton NLO corrections calculated in this work and similar terms with the twist-3 two parton NLO corrections calculated in Ref. [11] are present in the second column and the third column of Table III. Only  $P'$ ,  $\epsilon_T$ ,  $q_C$ , and  $\omega_C$  have significant differences between twist-3 two parton and twist-3 three parton calculations. The three parton penguin term  $P^{(3)} = 51.4\text{eV}$  has about 15.5% enhancement than the two parton  $P^{(2)} = 44.5\text{eV}$ . The most significant difference comes from the  $\epsilon_T$ . The three parton  $\epsilon_T^{(3)} = 14.6(\%)$  is about two third of the two parton  $\epsilon_T^{(2)} = 22.0(\%)$ . This

can be easily understood due to the enhanced effects from the three parton corrections, the denominator of Eq.(36) contains  $r_\chi(a_6 - \frac{1}{2}a_8)$ . The ratio  $r = (\epsilon_{3/2} - \epsilon_T)/\epsilon_T \sim C'/T'$  has been suggested to be an important index for distinguishing whether SM can or can not explain the puzzle. Let's compare the theoretically predicted values: the naive  $\epsilon_{3/2}(\%) = (22.7 \pm 7.0)_{th}$  and  $\epsilon_T(\%) = (14.6 \pm 4.0)_{th}$ , the improved  $\epsilon_{3/2}(\%) = (24.2 \pm 3.0)_{th}$  and  $\epsilon_T(\%) = (15.4 \pm 1.8)_{th}$ , and the averaged fit values,  $\epsilon_{3/2}(\%) = (24.3 \pm 1.1)_{fit}$  and  $\epsilon_T(\%) = (15.4 \pm 0.6)_{fit}$ , which result in

$$\begin{aligned} r_{fit} &\simeq (0.59 \pm 0.08)_{fit} \\ r_{th} &= (0.55 \pm 0.57)_{th}(Naive) \\ r'_{th} &= (0.57 \pm 0.24)_{th}(Improved) \end{aligned}$$

Due to the large uncertainties of the predictions, it is unable to use  $r_{th}$  to justify the SM. However, the improved  $r'_{th}$  and the fit  $r_{fit}$  imply that SM can explain the puzzle with  $2\sigma$  and  $7.4\sigma$ , respectively. For reference, the two parton prediction gives  $r^{(2)} \simeq 0.2$  as calculated from the second column of Table III, the values quoted from Ref. [11].

As for  $q$ , the three parton  $q^{(3)} = 0.33$  is about four times the two parton  $q^{(2)} = 0.083$ . The three parton predictions can accommodate the data without additional EW penguin contributions from other sources as the two parton predictions required. On the other hand, the three parton  $\omega_C^{(3)} = -7.9^\circ$  is about one sixth of the two parton

Table III. Perturbative parts of amplitude parameters are calculated at  $\mu_0 = 4.2^{+4.2}_{-2.1}$ ,  $\mu_1 = (4.6 \pm 0.3)$ ,  $\mu_2 = (5.3^{+0.5}_{-0.4})$ ,  $\mu_3 = (5.6 \pm 0.3)$ ,  $\mu_4 = (4.4^{+0.4}_{-0.3})$ ,  $\mu_{av} = (5.0 \pm 1.4)$ . The unit is in GeV. For simplicity, only central values are given for  $\mu_i$ ,  $i = 1, \dots, 4$ . The similar calculations up-to twist-3 two parton NLO quoted from Ref.[11] are listed for comparisons. The  $\dagger$  term is calculated by using the values given in Ref.[11].

parameters	$\mu_0$	Ref[11]	$\mu_1$	$\mu_2$	$\mu_3$	$\mu_4$	$\mu_{av}$
$ P' (\text{eV})$	$51.4^{+16.1}_{-10.3}$	$44.5^\dagger$	50.0	47.7	46.7	50.6	$48.8^{+6.0}_{-3.7}$
$\epsilon_a(\%)$	$1.9 \pm 0.1$	$1.9 \pm 0.1$	1.9	1.9	1.9	1.9	$1.9 \pm 0.1$
$\epsilon_{3/2}(\%)$	$22.7^{+7.0}_{-6.4}$	$25.7 \pm 4.8$	23.5	24.9	25.6	23.2	$24.2^{+2.5}_{-3.1}$
$\epsilon_T(\%)$	$14.6^{+4.0}_{-3.6}$	$22.0 \pm 3.6$	15.0	15.8	16.0	14.8	$15.4^{+1.4}_{-1.8}$
$q(\%)$	$60.1^{+0.4}_{-4.4}$	$58.8 \pm 6.7$	60.2	60.4	60.4	60.2	$60.5^{+0.2}_{-0.8}$
$q_C(\%)$	$31.6^{+3.2}_{-10.2}$	$8.3 \pm 4.9$	32.2	33.1	33.5	32.0	$33.0^{+1.6}_{-3.0}$
$\hat{\phi}_a(\text{deg})$	$21.5^{+1.2}_{-2.5}$	$16.6 \pm 5.2$	21.3	20.8	20.6	21.4	$20.9^{+1.1}_{-1.0}$
$\hat{\phi}(\text{deg})$	$-10.2^{+2.3}_{-1.7}$	$-10.2 \pm 4.1$	-10.4	-10.8	-11.0	-10.3	$-10.6^{+0.9}_{-0.6}$
$\hat{\phi}_T(\text{deg})$	$-6.8^{+3.8}_{-2.6}$	$-6.2 \pm 4.6$	-7.2	-7.8	-8.0	-7.0	$-7.5^{+1.5}_{-1.0}$
$\omega(\text{deg})$	$0.4^{+0.4}_{-0.7}$	$-2.5 \pm 2.8$	0.5	0.6	0.6	0.5	$0.5 \pm 0.2$
$\omega_C(\text{deg})$	$-9.3^{+4.4}_{-12.8}$	$-54.2 \pm 44.2$	-8.6	-7.5	-7.1	-8.0	$-7.9^{+1.7}_{-3.2}$

Table IV. Predictions and experimental data for branching ratios and direct CP asymmetries.

Decay modes	Naive	Improved	S4[30]	pQCD[14]	Fit	PDG2016	HFAG2016
$Br(B^- \rightarrow \pi^- \bar{K}^0)$	$25.1^{+18.2}_{-9.0}$	$22.6^{+5.9}_{-3.3}$	20.3	$21.5^{+8.0}_{-6.1}$	$23.9^{+0.8+0.0}_{-0.9-0.2}$	$23.7 \pm 0.8$	$23.79 \pm 0.75$
$A_{CP}(B^- \rightarrow \pi^- K_s^0)$	$1.3 \pm 0.1$	$1.3 \pm 0.0$	0.3	$0.38^{+0.097}_{-0.140}$	$-1.7^{+0.0+1.7}_{-0.0-1.9}$	$-1.7 \pm 1.6$	$-1.7 \pm 1.6$
$Br(B^- \rightarrow \pi^0 K^-)$	$14.7^{+9.1}_{-4.7}$	$13.5^{+3.0}_{-5.1}$	11.7	$12.5^{+4.5}_{-3.4}$	$13.1^{+0.5+0.0}_{-0.6-0.1}$	$12.9 \pm 0.5$	$12.94^{+0.52}_{-0.51}$
$A_{CP}(B^- \rightarrow \pi^0 K^-)$	$7.8^{+2.9}_{-2.6}$	$8.4^{+1.0}_{-1.3}$	-3.6	$2.2 \pm 2.1$	$3.6^{+0.3+2.5}_{-0.2-2.5}$	$3.7 \pm 2.1$	$4.0 \pm 2.1$
$Br(\bar{B}^0 \rightarrow \pi^+ K^-)$	$23.6^{+15.9}_{-8.1}$	$21.4^{+5.2}_{-3.0}$	18.4	$17.7^{+6.4}_{-4.9}$	$19.9^{+0.5+0.0}_{-0.6-0.0}$	$19.6 \pm 0.5$	$19.57^{+0.53}_{-0.52}$
$A_{CP}(\bar{B}^0 \rightarrow \pi^+ K^-)$	$4.4^{+2.3}_{-2.0}$	$4.9^{+0.8}_{-1.1}$	-4.1	$-6.5 \pm 3.1$	$-8.2^{+0.0+0.7}_{-0.0-0.7}$	$-8.2 \pm 0.6$	$-8.2 \pm 0.6$
$Br(\bar{B}^0 \rightarrow \pi^0 \bar{K}^0)$	$10.2^{+7.9}_{-3.8}$	$9.2^{+2.5}_{-1.4}$	8.0	$7.4^{+2.7}_{-2.1}$	$10.0^{+0.5+0.4}_{-0.5-0.0}$	$9.9 \pm 0.5$	$9.93 \pm 0.49$
$A_{CP}(\bar{B}^0 \rightarrow \pi^0 K^0)$	$-3.4^{+1.4}_{-1.8}$	$-3.7^{+0.8}_{-0.7}$	0.8	$-7.9^{+0.9}_{-1.1}$	$-1.0^{+0.1+8.3}_{-0.1-12.3}$	$-1 \pm 10$	$-1 \pm 10$

$$\omega_C^{(2)} = -54^\circ.$$

## B. Predictions

*a. Power Counting Puzzle* In literature, the simple version of the  $B \rightarrow \pi K$  puzzle is based on the analysis for the predictions of the SM by means of a power counting of the amplitude parameters [25, 41, 48, 49]. Under the standard parametrization of the CKM matrix elements, we have  $\lambda_u \sim O(\lambda^4)$  and  $\lambda_c \sim O(\lambda^2)$ , where  $\lambda = 0.22$  is the sine of the Cabibbo angle. If the  $SU(3)$  flavor symmetry is valid, then we have  $\epsilon_a \sim \epsilon_{KM} \sim O(\lambda^2)$ ,  $\epsilon_{3/2} \sim \epsilon_T \sim O(\lambda)$ ,  $q \sim q_C \sim 1$ ,  $\epsilon_{3/2} - \epsilon_T \sim O(\lambda^2)$  [25, 41, 48, 49]. Combining these facts, we have the following Standard Model (SM) predictions  $A_{CP}(B^- \rightarrow \pi^0 K^-) = A_{CP}(\bar{B}^0 \rightarrow \pi^+ K^-) \sim O(\lambda)$  and a vanishing  $\Delta_{th} A_{CP} = 0$  up-to  $O(\lambda^2)$ , if the strong phases are of similar orders,  $\phi \sim \phi_T$ ,  $\omega \sim \omega_C$  [5].

Because the  $\Delta A_{CP}$  is about  $O(\lambda)$ , at which SM predicts a vanishing  $\Delta A_{CP}$  with errors  $O(\lambda^2)$ . However, the direct CP asymmetries of four processes are all of  $O(\lambda^2)$ . Therefore, in order to reveal the mystery of the puzzle, it needs the calculation accuracy up-to  $O(\lambda^2)$

By order of magnitudes, the twist-3 power corrections are of  $O(\Lambda/m_B) \sim O(\lambda^2)$  and the NLO  $\alpha_s$  corrections are of  $O(\alpha_s^2(m_b)) \sim O(\lambda^2)$ . This implies that QCDF with complete twist-3 power corrections and NLO corrections has the precision of  $O(\lambda^2)$ . That ensures that our calculations are able to distinguish the different terms of the asymmetries. As a result, we may be able to figure out the crucial differences which lead to the puzzle.

To make the above explanation clear, let's separately calculate the four terms in the square bracket of each direct CP asymmetry in Eqs. (11-14). The results are present in Table V, the columns 1,  $\dots$ , 4, denote the j-th term of each  $A_{CP}$  equation. For  $A_{CP}(\pi^0 K^0)$ , the terms are separated by different lines. Now, we may understand why the puzzle may not exist:

1. Although  $\epsilon_a$  is much smaller than  $P'$ , but it should not be neglected for  $A_{CP}$ .
2. Most of the first and second terms are of  $O(\lambda^2)$  and the third and fourth terms of  $O(\lambda^3)$ . The largest term is  $-\epsilon_{3/2} \sin(\phi) \sin(\gamma)$  of  $A_{CP}(\pi^0 K^-)$ . The second large term is  $-\epsilon_T \sin(\phi_T) \sin(\gamma)$  of  $A_{CP}(\pi^+ K^-)$ . Both terms have different signs and magnitudes.

Table V. With the fit data, the different parts of the parametrization for the direct CP asymmetries are calculated. The index  $i$  is used to denote the decay modes:  $i = 1$  for  $B^- \rightarrow \pi^- K^0$ ,  $i = 2$ , for  $B^- \rightarrow \pi^0 K^-$ ,  $i = 3$  for  $\bar{B} \rightarrow \pi^- K^+$ , and  $i = 4$  for  $\bar{B}^0 \rightarrow \pi^0 K^0$ . The other columns are referred to the text.

$i$	$N_i$	1st term ( $10^{-3}$ )	2nd term ( $10^{-3}$ )	3rd term ( $10^{-3}$ )	4th term ( $10^{-3}$ )	$A_{CP}(10^{-3})$
1	1.98	-8.7	0	0	0	-17.2
2	1.65	-8.8	31.9	-1.0	0.4	36.9
3	1.94	-18.0	-21.9	-1.0	-1.0	-81.3
4	2.25	-8.3	-0.8	1.6	2.0	-12.3

Table VI. Experimental data and the QCDF predictions for ratios  $R$ ,  $R_c$ ,  $R_n$ .

Observable	2007[9]	2016[4]	Fit	S4	Naive	Improved
$R$	$0.89 \pm 0.04$	$0.89 \pm 0.05$	$0.87 \pm 0.04$	0.89	$0.92 \pm 0.67$	$0.91 \pm 0.26$
$R_c$	$1.10 \pm 0.07$	$1.09 \pm 0.06$	$1.10 \pm 0.07$	1.15	$1.17 \pm 1.12$	$1.19 \pm 0.55$
$R_n$	$1.00 \pm 0.07$	$0.99 \pm 0.06$	$1.00 \pm 0.06$	1.15	$1.16 \pm 1.19$	$1.16 \pm 0.42$

3. The puzzle assumes  $N_2 = N_3 = 2$ , but, in fact,  $N_2 = 1.65$  and  $N_3 = 1.94$ . It shows that the puzzle is incorrect.
4. The puzzle assumes the  $SU(3)$  flavor symmetry  $SU(3)_f$ , which requires  $\epsilon_{3/2}$  and  $\epsilon_T$  to have the same order of magnitudes. Naively, they would be equal if  $SU(3)_f$  is restrict. However,  $SU(3)_f$  is not conserved as the observed branching ratios show. Therefore,  $\epsilon_{3/2}$  and  $\epsilon_T$  would be different. The three parton calculations give  $\epsilon_{3/2}^{(3)} \simeq 1.6\epsilon_T^{(3)}$  while the two parton calculations have  $\epsilon_{3/2}^{(2)} \simeq 1.2\epsilon_T^{(2)}$ .

In summary, the power counting puzzle has accuracy of  $O(\lambda)$ . The  $SU(3)_f$  needs to be broken to explain the  $\Delta A_{CP} \neq 0$ , which comes from the largest terms of  $A_{CP}(\pi^0 K^-)$  and  $A_{CP}(\pi^+ K^-)$  being unequal and opposite signs. Although the power counting can correctly account for the magnitudes of these two terms of  $O(\lambda)$ , but it is unable to correctly distinguish their signs. From

this respect, the puzzle is solved by the broken  $SU(3)_f$ .

*b. Mixing Induced CP Asymmetry* We now test our MQCDF model to make a prediction for the mixing induced CP asymmetry  $S_{\pi^0 K_S} = 0.58 \pm 0.06$  [4]. Under the invariance of CPT, the time dependent CP asymmetry  $A_{CP}(t)$  for  $\bar{B}^0 \rightarrow \pi^0 K^0$  is given by [4]

$$A_{CP}(t) = \frac{\Gamma_{\bar{B} \rightarrow f}(t) - \Gamma_{B^0 \rightarrow f}(t)}{\Gamma_{\bar{B} \rightarrow f}(t) + \Gamma_{B^0 \rightarrow f}(t)} = \frac{-C_f \cos(\Delta m_d t) + S_f \sin(\Delta m_d t)}{\cosh(\frac{\Delta \Gamma_d}{2} t) + A_f^{\Delta \Gamma} \sinh(\frac{\Delta \Gamma_d}{2} t)},$$

where the  $B^0 - \bar{B}^0$  system has mass difference  $\Delta m_d$  and width difference  $\Delta \Gamma_d$  for the mass eigenstate  $|B^0\rangle$  and  $|\bar{B}^0\rangle$ . The quantities are given by

$$C_f = \frac{1 - |\lambda_f|^2}{1 + |\lambda_f|^2}, \quad S_f = \frac{2\text{Im}(\lambda_f)}{1 + |\lambda_f|^2}, \quad A_f^{\Delta \Gamma} = -\frac{2\text{Re}(\lambda_f)}{1 + |\lambda_f|^2},$$

where  $\lambda_f$  is defined as

$$\lambda_f = -e^{-2i\beta} \left[ \frac{(1 + \epsilon_a e^{i\phi_a} e^{-i\gamma} + (\epsilon_{3/2} e^{i\phi} - \epsilon_T e^{i\phi_T}) e^{-i\gamma} + (\epsilon_T q_C e^{i(\phi_T + \omega_C)} - \epsilon_{3/2} q e^{i(\phi + \omega)}))}{(1 + \epsilon_a e^{i\phi_a} e^{i\gamma} + (\epsilon_{3/2} e^{i\phi} - \epsilon_T e^{i\phi_T}) e^{i\gamma} + (\epsilon_T q_C e^{i(\phi_T + \omega_C)} - \epsilon_{3/2} q e^{i(\phi + \omega)}))} \right].$$

1. By using the world averaged  $\beta = (22.5 \pm 4.4 \pm 1.2 \pm 0.6)^\circ$ , the calculations give  $S_f = 0.57 \pm 0.13$  and  $C_f = -0.01$  and  $A_f^{\Delta \Gamma} = 0.82 \pm 0.09$ .
2. By using the above expression and the fitted parameters for  $\pi^0 K_S$  mode given in the column  $\mu_4$  of Table III, the fit to  $S_f = 0.58 \pm 0.06$  gives the fitted  $\beta = (22.92_{-2.13}^{+2.08})^\circ$ , which is in agreement with the world averaged  $\beta = (22.5 \pm 4.4 \pm 1.2 \pm 0.6)^\circ$ .

*c. Ratios of modes* Three famous ratios,  $R$ ,  $R_c$  and  $R_n$  have been widely used for demonstration of the  $B \rightarrow$

$\pi K$  puzzle. We now compare their theoretical ( $R^{th}$  in the Improved column) and experimental values ( $R^{exp}$  in the 2016 column) in Table VI, which are calculated according to the column Improved in Table IV and the experimental data, respectively.

From the above calculations, we may notice the following interesting points:

1. For the ratio  $R$ , the central value of the predicted value  $R^{th} = 0.91$  is very close to that of the experimental value  $R^{exp} = 0.89$  within 3%.

Table VII. Amplitudes calculated according to the Improved and Fit data. Only uncertainties from the scale variables  $\mu_{av}$  and  $\mu_i$ ,  $i = 1, \dots, 4$ , are included.

decay modes	Improved	Fit
$A(B^- \rightarrow \pi^- K^0)(\text{eV})$	$(49.4 \pm 6.0)e^{-i173^\circ}$	$(50.0 \pm 1.1)e^{-i173^\circ}$
$A(B^- \rightarrow \pi^0 K^-)(\text{eV})$	$(39.5 \pm 3.8)e^{i18^\circ}$	$(38.0 \pm 0.9)e^{i19^\circ}$
$A(\bar{B}^0 \rightarrow \pi^- K^+)(\text{eV})$	$(50.8 \pm 5.5)e^{i15^\circ}$	$(45.8 \pm 0.7)e^{i17^\circ}$
$A(\bar{B}^0 \rightarrow \pi^0 K^0)(\text{eV})$	$(31.9 \pm 4.2)e^{-i177^\circ}$	$(33.7 \pm 1.0)e^{-i179^\circ}$
$A(B^- \rightarrow \pi^- K^0) + \sqrt{2}A(B^- \rightarrow \pi^0 K^-)$	$(12.0 \pm 8.0)e^{i70^\circ}$	$(11.5 \pm 1.7)e^{i84^\circ}$
$A(\bar{B}^0 \rightarrow \pi^- K^+) + \sqrt{2}A(\bar{B}^0 \rightarrow \pi^0 K^0)$	$(11.5 \pm 8.0)e^{i70^\circ}$	$(13.1 \pm 1.6)e^{i107^\circ}$
$r$	$(1.04 \pm 1.0)e^{i0.4^\circ}$	$(0.87 \pm 0.15)e^{-i23^\circ}$

2. The ratio of central values show  $R_n^{th}/R_c^{th} \simeq 1+0.9\%$  and  $R_n^{exp}/R_c^{exp} = 1+9.2\%$ . Both are compatible within 10% despite of their respective uncertainties. The discussion about the 10% difference is left to the Sec.VI.

In summary, the comparisons between the theoretical predictions of this work and the experimental data for these three famous ratios show no similar large discrepancies as claimed in [5–7].

### C. Comparisons With Other Approaches

*a. Flavor symmetry approach* Many studies have employed the flavor symmetry approach [5–7, 10, 22, 23, 42, 48, 50–54], which is an extension of the isospin symmetry approach. The amplitudes are expressed in terms of parameters which satisfy the symmetry. To conserve the symmetry, the parameters would be process-independent. By means of many sophisticated arguments, many important insights for the flavor physics have been derived. The arguments heavily rely on the argument that the common parameters involved in different processes are universal such that they can be used for predictions. However, these arguments would be questionable if the parameters are process-dependent according to our founding in this work.

*b. Global-fit approach* In literature, there have been some studies [9, 24, 25] by employing the global-fit for analysis. These studies have been continuing to insist the existence of the  $B \rightarrow \pi K$  puzzle. The basic assumption of this fitting approach is that there would exist some symmetries within the amplitudes such that the amplitudes can be parameterized in terms of some universal variables. However, this method has its intrinsic uncertainties. Since there exist many (perhaps infinite) possible best-fit results, it is difficult to distinguish which result is correct. In our approach, there is no such problem.

*c. NLO PQCD approach* Similar studies have been made by employing the PQCD approach [13–15]. The complete NLO calculations [14] are improved than the partial NLO ones [15]. The complete NLO predictions [14] for the branching ratios and direct CP asymmetries

are compatible with the experimental data. The authors of Ref. [13] indicated that some nonperturbative strong phase from the Glauber gluons are necessary. Although the QCDF and the PQCD approaches are based on different factorization assumptions, their calculations up-to NLO and twist-3 order agree within theoretical uncertainties.

*d. QCDF with final state interactions* The final state interactions of the  $B \rightarrow \pi K$  decays are introduced to account for strong phases (see e.g. [27]). This approach uses the QCDF predictions as the reference by adding the final state interaction effects. The final state interactions occur through long distance inferences between different final states. The calculations introduce nonperturbative parameters which are determined by a best-fit to the data. Since the QCDF calculations contain final state interactions in the  $a_i$  functions, there would exist double counting effects in this approach [30]. On the other hand, our model has avoided this problem.

*e. QCDF with endpoint divergences* There exist endpoint divergent terms in the standard QCDF calculations. To regularize the divergences, the following model is introduced [30]

$$X_A = (1 + \rho_A e^{i\phi_A}) \ln\left(\frac{m_B}{\Lambda_h}\right); \quad \rho_A \leq 1, \quad \Lambda_h = 0.5\text{GeV}.$$

The parameters  $\rho_A$  and  $\phi_A$  are determined by a global-fit to the data. Because the factorization formula Eq.(20) is free from these end-point divergences [45], no such terms need to be considered in our calculations. Since the phase  $\phi_A$  is associated with the annihilation terms, the explanations for the puzzle are different from ours.

### D. Isospin Symmetry Breaking

*a. Broken isospin symmetry* The isospin symmetry is assumed conserved under the weak interactions. The  $B \rightarrow \pi K$  amplitudes would obey the quadrangle relation Eq.(6)[20, 49] This relation leads to the ratio  $R_c/R_n = 1$ , which is shown by the central value of the QCDF prediction (the Improved)  $R_c/R_n \simeq 1$ VI. However, the central values of the last experimental data show that  $R_c/R_n = 1.1 > 1$ . How does this imply for the quad-

angle relation? To answer this, we may calculate the following ratio for the amplitudes listed in Table VII

$$r = \frac{A(\pi^- K^0) + \sqrt{2}A(\pi^0 K^-)}{A(\pi^- K^+) + \sqrt{2}A(\pi^0 K^0)} = \frac{A_{3/2}(B^-)}{A_{3/2}(\bar{B}^0)},$$

$$r_{exp} = (0.87 \pm 0.15)e^{-i23^\circ},$$

$$r_{th} = (1.04 \pm 1.0)e^{i0.4^\circ},$$

where  $r_{exp}$  is calculated by the Fit column in Table VII and the  $r_{th}$  is calculated by the Improved column in the same table. The experimental data imply that the amplitudes would not obey the quadrangle relation. It is in contradiction to the theoretical assumption,  $r_{exp} \neq r_{th}$ . Within uncertainties, we obtain  $r_{exp} \neq 1$  at  $6\sigma$  significance. That is  $A_{3/2}(B^-) \neq A_{3/2}(\bar{B}^0)$ . Similar result can be obtained by the  $B_{1/2}$  or  $A_{1/2}$ . This shows that isospin symmetry needs to be broken for explaining the data. Otherwise, the puzzle would remain. In other words, the  $B \rightarrow \pi K$  puzzle is solved by the broken isospin symmetry.

The isospin symmetry is broken by (i) the process dependent factorization scale  $\mu_i$ , and (ii) the process-dependent non-vanishing nonperturbative phases  $\bar{\phi}_a, \bar{\phi}, \bar{\phi}_T$ .

It is interesting to note that the mass differences  $\Delta m_q = |m_d - m_u| \simeq 2.5\text{MeV}$  with  $m_{u(d)}$  the up (down) quark's mass,  $\Delta m_\pi = |m_{\pi^0} - m_{\pi^\pm}| \simeq 5\text{MeV}$  with  $m_{\pi^0(\pi^\pm)}$  the pion's mass,  $\Delta m_K = |m_{K^0} - m_{K^\pm}| \simeq 4\text{MeV}$  with  $m_{K^0(K^\pm)}$  the kaon's mass, or  $\Delta m_B = |m_{B^0} - m_{B^\pm}| \simeq 0.3\text{MeV}$  with  $m_{B^0(B^\pm)}$  the  $B^{0(\pm)}$  meson's mass can also break the isospin symmetry. The largest effect comes from the mass difference,  $\Delta m_\pi \simeq 5\text{MeV}$  or  $\Delta m_K \simeq 4\text{MeV}$ , which contribute about  $5 \times 10^{-5}$  of the ratio  $r$ .

To distinguish, we call the former as the “dynamic” isospin symmetry breaking and the latter as the “static”.

*b. Nonperturbative Strong Phases* The three non-perturbative strong phases  $\bar{\phi}_a, \bar{\phi}, \bar{\phi}_T$  have a specific pattern in  $B \rightarrow \pi K$  system as shown in Table. II. The full strong phases,  $\phi_a = \hat{\phi}_a + \bar{\phi}_a$ ,  $\phi = \hat{\phi} + \bar{\phi}$ ,  $\phi_T = \hat{\phi}_T + \bar{\phi}_T$ , represent the long distance final state interactions. The absolute values of these phases indicate that  $|\phi_a| > |\phi| \simeq |\phi_T|$ . A large negative  $\phi_a$  is observed. Since these three phases are closely related to the weak angle  $\gamma$ , three phases could be redefined as  $\Phi_a = \phi_a - \gamma$ ,

$\Phi = \phi - \gamma$ ,  $\Phi_T = \phi_T - \gamma$ . From this respect, there exist three possibilities

1. The puzzle is solved by SM, if the phase factors  $\phi_a, \phi, \phi_T$  are completely of strong interactions.
2. The puzzle is solved by NP, if the phase factors  $\Phi_a, \Phi, \Phi_T$  completely come from NP effects.
3. Both of 1 and 2 are possible.

The  $B \rightarrow \pi K$  puzzle is resolved by SM if the phase factors are completely of strong interactions. On the other hand, if the puzzle is due to NP effects. The phase factors would be signals of NP physics. The  $B \rightarrow \pi K$  puzzle is reduced to find the NP explanations for the three extracted phases. Since we are unable to distinguish the above two scenarios, there exists a third solution that both SM and NP effects coexist in our solutions. To clarify which scenario is correct relies on future studies.

## VI. CONCLUSION

In this work, we have developed an effective method for analyzing the  $B \rightarrow \pi K$  system by using the MQCDF model. The crucial roles are played by the phase factors  $\bar{\phi}_a, \bar{\phi}, \bar{\phi}_T$ . By the fitting strategy, we may determine their values definitely. It was found that their values depend on the decay modes. It is possible to extract a universal  $\gamma$  from the data, whose value is in good agreement with the world averaged value. The fit result was used to extract the weak angle  $\beta$  from the mixing induced CP asymmetry  $S_{\pi^0 K_S^0}$ . The extracted  $\beta$  is in a good agreement with the world averaged value. From these evidences, our proposed model could completely solve the original puzzle defined in Sec.I.

By using the fit data, the model was able to reconstruct the experimental data at the amplitude level as shown in Table VII. This implies that the isospin symmetry of the  $B \rightarrow \pi K$  system would be broken dynamically by strong interactions. In other words, the  $B \rightarrow \pi K$  puzzle is solved by this dynamical isospin symmetry breaking.

It is possible to generalize our model by introducing more free hadronic parameters to account for any NP effect. The application of our method to other decay processes is straightforward.

---

[1] M. Battaglia, A. J. Buras, P. Gambino, A. Stocchi, D. Abbaneo, A. Ali, P. Amaral, V. Andreev, M. Artuso, E. Barberio, et al., ArXiv High Energy Physics - Phenomenology e-prints (2003), hep-ph/0304132.  
[2] A. J. Buras, ArXiv High Energy Physics - Phenomenology e-prints (2005), hep-ph/0505175.  
[3] A. J. Bevan, B. Golob, T. Mannel, S. Prell, B. D. Yabsley, H. Aihara, F. Anulli, N. Arnaud, T. Aushev, M. Beneke, et al., European Physical Journal C **74**, 3026 (2014),

1406.6311.  
[4] C. Patrignani et al. (Particle Data Group), Chin. Phys. **C40**, 100001 (2016).  
[5] A. J. Buras, R. Fleischer, S. Recksiegel, and F. Schwab, Phys. Rev. Lett. **92**, 101804 (2004), hep-ph/0312259.  
[6] A. J. Buras, R. Fleischer, S. Recksiegel, and F. Schwab, Eur. Phys. J. **C32**, 45 (2003), hep-ph/0309012.  
[7] A. J. Buras, R. Fleischer, S. Recksiegel, and F. Schwab, Nucl. Phys. **B697**, 133 (2004), hep-ph/0402112.

- [8] S. Khalil, Phys. Rev. **D72**, 035007 (2005), hep-ph/0505151.
- [9] S. Baek and D. London, Phys. Lett. **B653**, 249 (2007), hep-ph/0701181.
- [10] R. Fleischer, S. Jager, D. Pirjol, and J. Zupan, Phys. Rev. **D78**, 111501 (2008), 0806.2900.
- [11] M. Beneke, G. Buchalla, M. Neubert, and C. Sachrajda, Nuclear Physics B **606**, 245 (2001), ISSN 0550-3213, URL <http://www.sciencedirect.com/science/article/pii/S0550321301002516>.
- [12] Y. Y. Keum, H.-N. Li, and A. I. Sanda, Phys. Rev. **D63**, 054008 (2001), hep-ph/0004173.
- [13] H.-N. Li and S. Mishima, Phys. Rev. D **83**, 034023 (2011), 0901.1272.
- [14] W. Bai, M. Liu, Y.-Y. Fan, W.-F. Wang, S. Cheng, and Z.-J. Xiao, Chinese Physics C **38**, 033101 (2014), 1305.6103.
- [15] H.-n. Li, S. Mishima, and A. I. Sanda, Phys. Rev. **D72**, 114005 (2005), hep-ph/0508041.
- [16] S. Khalil, A. Masiero, and H. Murayama, Phys. Lett. **B682**, 74 (2009), 0908.3216.
- [17] J. Charles, S. Descotes-Genon, V. Niess, and L. Vale Silva, Eur. Phys. J. **C77**, 214 (2017), 1611.04768.
- [18] Y. Amhis, S. Banerjee, E. Ben-Haim, F. Bernlochner, A. Bozek, C. Bozzi, M. Chrzęszcz, J. Dingfelder, S. Duell, M. Gersabeck, et al., The European Physical Journal C **77**, 895 (2017), ISSN 1434-6052, URL <https://doi.org/10.1140/epjc/s10052-017-5058-4>.
- [19] R. Orava and O. V. Selyugin (2018), 1804.05201.
- [20] Y. Nir and H. R. Quinn, Phys. Rev. Lett. **67**, 541 (1991).
- [21] M. Gronau, Phys. Lett. **B265**, 389 (1991).
- [22] M. Neubert, Journal of High Energy Physics **1999**, 014 (1999), URL <http://stacks.iop.org/1126-6708/1999/i=02/a=014>.
- [23] C.-W. Chiang, M. Gronau, J. L. Rosner, and D. A. Suprun, Phys. Rev. **D70**, 034020 (2004), hep-ph/0404073.
- [24] S. Baek, C.-W. Chiang, and D. London, Phys. Lett. **B675**, 59 (2009), 0903.3086.
- [25] N. B. Beaudry, A. Datta, D. London, A. Rashed, and J.-S. Roux, Journal of High Energy Physics **2018**, 74 (2018), ISSN 1029-8479, URL [https://doi.org/10.1007/JHEP01\(2018\)074](https://doi.org/10.1007/JHEP01(2018)074).
- [26] D. Du, J. Sun, D. Yang, and G. Zhu, Phys. Rev. D **67**, 014023 (2003), hep-ph/0209233.
- [27] H.-Y. Cheng, C.-K. Chua, and A. Soni, Phys. Rev. D **71**, 014030 (2005), hep-ph/0409317.
- [28] C. W. Bauer, I. Z. Rothstein, and I. W. Stewart, Phys. Rev. **D74**, 034010 (2006), hep-ph/0510241.
- [29] M. Beneke, G. Buchalla, M. Neubert, and C. T. Sachrajda, Physical Review Letters **83**, 1914 (1999), hep-ph/9905312.
- [30] M. Beneke and M. Neubert, Nuclear Physics B **675**, 333 (2003), hep-ph/0308039.
- [31] J. Collins, *Foundations of Perturbative QCD* (Cambridge, UK: Cambridge University Press, 2011).
- [32] J. C. Collins, D. E. Soper, and G. F. Sterman, Adv. Ser. Direct. High Energy Phys. **5**, 1 (1989), hep-ph/0409313.
- [33] M. Beneke, G. Buchalla, M. Neubert, and C. T. Sachrajda, Nuclear Physics B **591**, 313 (2000), hep-ph/0006124.
- [34] A. J. Buras and L. Silvestrini, Nuclear Physics B **569**, 3 (2000), hep-ph/9812392.
- [35] G. Bell, Nuclear Physics B **795**, 1 (2008), ISSN 0550-3213, 0705.3127, URL <http://www.sciencedirect.com/science/article/pii/S0550321307006888>.
- [36] M. Beneke, T. Huber, and X.-Q. Li, Nuclear Physics B **832**, 109 (2010), 0911.3655.
- [37] G. Bell, Nuclear Physics B **822**, 172 (2009), 0902.1915.
- [38] M. Neubert and B. D. Pecjak, Journal of High Energy Physics **2002**, 028 (2002), URL <http://stacks.iop.org/1126-6708/2002/i=02/a=028>.
- [39] G. Bell, M. Beneke, T. Huber, and X.-Q. Li, Physics Letters B **750**, 348 (2015), 1507.03700.
- [40] T.-W. Yeh, Chin. J. Phys. **46**, 535 (2008), 0802.1855.
- [41] M. Imbeault, A. Datta, and D. London, International Journal of Modern Physics A **22**, 2057 (2007), hep-ph/0603214.
- [42] M. Gronau, D. Pirjol, and T.-M. Yan, Phys. Rev. **D60**, 034021 (1999), [Erratum: Phys. Rev.D69,119901(2004)], hep-ph/9810482.
- [43] G. Buchalla, A. J. Buras, and M. E. Lautenbacher, Rev. Mod. Phys. **68**, 1125 (1996), hep-ph/9512380.
- [44] A. J. Buras, in *Probing the standard model of particle interactions. Proceedings, Summer School in Theoretical Physics, NATO Advanced Study Institute, 68th session, Les Houches, France, July 28-September 5, 1997. Pt. 1*, 2 (1998), pp. 281–539, hep-ph/9806471.
- [45] T.-W. Yeh, Chin. J. Phys. **46**, 649 (2008), 0712.2292.
- [46] William H. Press, Saul A. Teukolsky, William T. Vetterling, Brian P. Flannery, *Numerical Recipes (Third Edition)* (Cambridge University Press, 2010).
- [47] D. W. Marquardt, Journal of the Society for Industrial and Applied Mathematics **11**, 431 (1963), <https://doi.org/10.1137/0111030>, URL <https://doi.org/10.1137/0111030>.
- [48] M. Gronau, O. F. Hernández, D. London, and J. L. Rosner, Phys. Rev. D **52**, 6356 (1995), hep-ph/9504326.
- [49] M. Gronau, O. F. Hernández, D. London, and J. L. Rosner, Phys. Rev. D **52**, 6374 (1995), hep-ph/9504327.
- [50] D. Zeppenfeld, Z. Phys. **C8**, 77 (1981).
- [51] A. J. Buras and R. Fleischer, Physics Letters B **341**, 379 (1995), hep-ph/9409244.
- [52] A. J. Buras and R. Fleischer, Physics Letters B **360**, 138 (1995), hep-ph/9507460.
- [53] R. Fleischer and T. Mannel, Phys. Rev. D **57**, 2752 (1998), hep-ph/9704423.
- [54] M. Gronau and J. L. Rosner, Physics Letters B **572**, 43 (2003), hep-ph/0307095.